KADIR HAS UNIVERSITY
SCHOOL OF GRADUATE STUDIES
PROGRAM OF MATERIAL SCIENCE AND NANOTECHNOLOGY

# A SERIES OF 1,10-PHENANTHROLINE AND PRODIGIOSIN DERIVATIVES AS HIGHLY POTENT AND EFFECTIVE NEW ANTICANCER THERAPEUTIC DRUGS AGAINST mTOR AND HDAC1 ENZYMES

SÜMEYYE BERFİN GÜL

MASTER OF SCIENCE THESIS

İSTANBUL, FEBRUARY, 2024

# A SERIES OF 1,10-PHENANTHROLINE AND PRODIGIOSIN DERIVATIVES AS HIGHLY POTENT AND EFFECTIVE NEW ANTICANCER THERAPEUTIC DRUGS AGAINST mTOR AND HDAC1 ENZYMES

SÜMEYYE BERFİN GÜL
ADVISOR: ASST. PROF. M. MUSTAFA ÇETİN

A thesis submitted to
the School of Graduate Studies of Kadir Has University
in partial fulfilment of the requirements for the degree of
Master of Science in
Material Science and Nanotechnology

İstanbul, February, 2024

# APPROVAL

A SERIES OF 1,10-PHENANTHROLINE AND PRODIGIOSIN DERIVATIVES AS HIGHLY POTENT AND EFFECTIVE NEW ANTICANCER THERAPEUTIC DRUGS AGAINST mTOR AND HDAC1 ENZYMES submitted by SÜMEYYE BERFİN GÜL, in partial fulfillment of the requirements for the degree of Master of Science in Material Science and Nanotechnology is approved by

Asst. Prof., M. Mustafa Çetin (Advisor) ……..
Kadir Has University

Prof. Dr., Kemal Yelekçi ……..
Kadir Has University

Prof. Dr., Emrah Çakmakçı ……..
Marmara University

Asst. Prof., Emin İstif ……..
Kadir Has University

Doc. Dr., Safacan Kölemen ……..
Koç University

I confirm that the signatures above belong to the aforementioned faculty members.

_____

Prof. Dr., Mehmet Timur Aydemir
Director of the School of Graduate Studies
Date of Approval: 01.02.2024

**DECLARATION ON RESEARCH ETHICS AND PUBLISHING METHODS**

I, SÜMEYYE BERFİN GÜL; hereby declare

- that this Master of Science Thesis that I have submitted is entirely my own work and I have cited and referenced all material and results that are not my own in accordance with the rules;
- that this Master of Science Thesis does not contain any material from any research submitted or accepted to obtain a degree or diploma at another educational institution;
- and that I commit and undertake to follow the "Kadir Has University Academic Codes of Conduct" prepared in accordance with the "Higher Education Council Codes of Conduct".

In addition, I acknowledge that any claim of irregularity that may arise in relation to this work will result in a disciplinary action in accordance with the university legislation.

SÜMEYYE BERFİN GÜL

_____

Date (01/02/2024)

*To My Dearest Family...*

# ACKNOWLEDGEMENT

I would like to express my sincere gratitude to my advisor, Asst. Prof. M. Mustafa Çetin, for his invaluable guidance and support throughout my research endeavors. Being a part of the SOPR Lab has been a rewarding experience, and I extend my thanks to the lab members for their collaboration and contributions.

Additionally, I want to convey my appreciation to Prof. Dr. Kemal Yelekçi and his student Damla Dere for their support and insightful input. This research would not have been possible without the collective efforts and encouragement from these individuals.

Also, I want to sincerely thank my friends and family for their constant encouragement and support during this research journey. Their understanding, encouragement, and belief in my pursuits have been a constant source of inspiration. Their presence has made this endeavor more meaningful, and I am truly grateful for their enduring support. I am deeply grateful for your love and support. Thank you for being a part of my life.

Moreover, I would like to express my sincere appreciation to my fiance, Taha Yüceler, for his unwavering love, support, and understanding throughout this research. His encouragement, patience, and belief in my efforts have been a source of strength and motivation. I am grateful for his presence and the positive impact he has had on both my personal and academic life. Thank you, Taha, for being a constant source of support and inspiration.

Finally, I sincerely appreciate Kadir Has University, The Graduate School and Materials Science and Nanotechnology MSc Program for their support and scholarship opportunity for my MSc education here at KHAS.

A SERIES OF 1,10-PHENANTHROLINE AND PRODIGIOSIN DERIVATIVES AS HIGHLY POTENT AND EFFECTIVE NEW ANTICANCER THERAPEUTIC DRUGS AGAINST mTOR AND HDAC1 ENZYMES

# ABSTRACT

Breast cancer is considered the second type of cancer with the highest probability of brain metastasis. However, there is no efficient anticancer therapeutic/treatment specific for this type of cancer. Therefore, there is a growing need for the creation of novel and effective anticancer therapeutic drugs/APIs that inhibit the enzymes, mTOR and HDAC, crucial in the progression of breast cancer. The present study has examined the structure-activity relationship and in silico modeling of a range of prodigiosin and 1,10-phenanthroline derivatives as novel and highly potent anticancer therapeutic drugs/APIs targeting mTOR and HDAC enzymes. Comparative analysis with the natural product Ps was performed to identify highly potent ligands. MD simulations of these ligands have been performed, and from the trajectory of the MD simulations, the RMSD, RMSF, and Rg parameters were computed to assess structural conformations, stability, flexibility/fluctuation, and overall dimensions of ligand-enzyme complexes. Additionally, an ADMET study, adhering to Lipinski's rule of five, evaluates pharmacological potential. 20 of the highly potent ligands, especially **2a, 6b, 13, and 13a**, demonstrate promising binding energies ranging from -9.4 to -7.1 kcal/mol and inhibition constants ranging from 225 to 569 nM against HDAC1 and/or mTOR enzymes when compared to the natural product Ps. Significantly, ligands **2a, 5, 6b, 7b, and 13** exhibit effective dual action against both enzymes. Furthermore, according to the ADMET study, none of the selected ligands have violated more than two of the Lipinski's rule of five criteria, indicating a very promising potential to be pharmacologically active. As a result, we have obtained certain compounds using in silico computational modeling that offer exceptional therapeutic potential for breast cancer patients who also have a high risk of brain metastasis. Further syntheses of a few selected compounds are currently being investigated in our laboratories due to the extremely encouraging results.

**Keywords:** Anticancer therapeutic drugs/APIs, breast cancer brain metastases, mTOR, HDAC, 1,10-phenanthroline, prodigiosin

mTOR VE HDAC1 ENZİMLERİNE KARŞI YÜKSEK GÜÇLÜ VE ETKİLİ YENİ ANTİKANSER TERAPÖTİK İLAÇLAR OLARAK 1,10-FENANTROLİN VE PRODİGİOSİN TÜREVLERİ SERİSİ

# ÖZET

Meme kanseri, beyin metastazı olasılığı en yüksek olan ikinci kanser türü olarak kabul edilmektedir. Ancak bu kanser türüne özgü etkili bir antikanser terapötik/tedavisi mevcut değildir. Bu nedenle, meme kanserinin ilerlemesinde hayati önem taşıyan mTOR ve HDAC enzimlerini inhibe eden yeni ve etkili antikanser terapötik ilaçların/API'lerin oluşturulmasına yönelik artan bir ihtiyaç vardır. Bu çalışma, mTOR ve HDAC enzimlerini hedef alan yeni ve oldukça güçlü antikanser terapötik ilaçlar/API'ler olarak bir dizi prodigiosin ve 1,10-fenantrolin türevlerinin yapı-aktivite ilişkisini ve in silico modellemesini incelemiştir. Oldukça güçlü ligandları tanımlamak için doğal ürün Ps ile karşılaştırmalı analiz yapılmıştır. Bu ligandların MD simülasyonları gerçekleştirilmiş ve MD simülasyonlarının yörüngesinden, ligand-enzim komplekslerinin yapısal konformasyonlarını, stabilitesini, esnekliğini/dalgalanmasını ve genel boyutlarını değerlendirmek için RMSD, RMSF ve Rg parametreleri hesaplanmıştır. Ek olarak, Lipinski'nin beş kuralı ile yapılan ADMET çalışması farmakolojik potansiyeli değerlendirmektedir. Doğal ürün Ps ile karşılaştırıldığında, oldukça güçlü ligandlardan 20'si, özellikle **2a, 6b, 13 ve 13a**, HDAC1 ve/veya mTOR enzimlerine karşı, -9,4 ila -7,1 kcal/mol arasında değişen umut verici bağlanma enerjileri ve 225 ila 569 nM arasında değişen inhibisyon sabitleri sergiler. Özellikle, **2a, 5, 6b, 7b ve 13** numaralı ligandlar, her iki enzime karşı etkili ikili etki sergiler. Ayrıca ADMET çalışmasına göre, seçilen ligandların hiçbiri Lipinski'nin beş kriterli kuralından ikiden fazlasını ihlal etmedi; bu da farmakolojik olarak aktif olma potansiyelinin çok umut verici olduğunu gösterdi. Sonuç olarak, in silico hesaplamalı modellemeyi kullanarak, aynı zamanda beyin metastazı riski yüksek olan meme kanseri hastaları için olağanüstü terapötik potansiyel sunan belirli bileşikler elde ettik. Son derece umut verici sonuçlar nedeniyle, seçilmiş birkaç bileşiğin daha ileri sentezleri şu anda laboratuvarlarımızda araştırılmaktadır.

**Anahtar Sözcükler:** Antikanser tedavi edici ilaçlar/API'ler, meme kanseri beyin metastazları, mTOR, HDAC, 1,10-fenantrolin, prodigiosin

# TABLE OF CONTENTS

# LIST OF FIGURES

# LIST OF TABLES

# LIST OF SYMBOLS

| | |
|---|---|
| Å | Angstrom |
| Δ | Delta |
| μM | Micromolar |
| nM | Nanomolar |
| ns | Nanosecond |

# LIST OF ACRONMYMS AND ABBREVIATIONS

| | |
|---|---|
| 2D | Two-dimensional |
| 3D | Three-Dimensional |
| ADT | AutoDock Tools |
| API | Active Pharmaceutical Ingredients |
| HDAC | Histone Deacetylases |
| IL-8 | Interleukin-8 |
| $K_i$ | Inhibition Constant |
| LogP | Partition Coefficient |
| MD | Molecular Dynamics |
| mTOR | Mammalian Target of Rapamycin |
| MW | Molecular Weight |
| NAMD | Nanoscale Molecular Dynamics |
| PHEN | 1,10-Phenanthroline |
| PI3Ks/AKT | Phosphatidylinositol-3-kinases |
| Ps | Prodigiosin |
| PSA | Polar Surface Area |
| Rg | Radius of Gyration |
| RMSD | Root-Mean-Square Deviations |
| RMSF | Root-Mean-Square Fluctuation |
| SAR | Structure-Activity Relationship |
| SERDs | Selective Estrogen Receptor Degraders |
| TNBC | Triple Negative Breast Cancer |

# 1. INTRODUCTION

The attributed deaths of approximately 17% is due to the second leading cause cancer for the world population [1], where breast cancer counts for 25% of all cases [2]. Breast cancer is considered to be the most common type of cancer in females, with the second-highest probability of brain metastasis [3,4]. In approximately 10-20% of patients diagnosed with breast cancer, malignant brain metastasis was also found [5,6]. In recent years, this percentage is continuously increasing with the development of diagnostic and prognostic methods [7] in the healthcare system and technology. Most research in breast cancer is currently directed into the mortality of breast cancer brain metastasis with the development of therapeutics and prognostic tools [8]. Alternative tools and treatments are investigated due to the development of resistance causing brain metastasis, epigenetic changes and several mutations, and individual differences in response to treatments [9]. However, there is no effective treatment or cancer-specific therapeutics, especially for patients with a high risk of brain metastasis. Hence, there is an increasing demand in the field to develop highly efficient breast cancer drugs that inhibit the enzymes that are crucial in the modulation of breast cancer.

Current surgical treatment of breast cancer is based on partial or complete removal of the diseased organ and axillary dissection. These treatment methods allow for both local treatment of the disease and understanding the stage of the tumor, as well as deciding whether auxiliary treatment is necessary. The main purpose of cancer treatments is to ensure recovery by clearing malignant cells and leaving the remaining cells as intact as possible, or if this is not possible then to extend the life and increase the quality of life for the person who has cancer. Treatment methods include surgery, systematic treatments and radiation therapy. These methods can be used both alone and in combination to treat breast cancer [10, 11]. Breast cancer is a metastatic cancer and can often spread to distant organs such as bones, liver, lungs and brain. Early diagnosis of the disease provides improved prognosis and high survival [12]. There are numerous risk factors in the development of breast cancer, such as gender, gene mutations, family history, age, estrogen and lifestyle [13]. Each person's cancer risk is a combination of different factors.

Lifestyle, our genes and the environment we live in are the biggest factors that increase or decrease the risk of getting cancer. It may not always be possible to avoid these risk factors. For instance, having certain genes makes breast cancer more likely to occur even if a person avoids from smoking [14]. In breast cancer, increasing protective factors such as understanding carcinogenesis, investigating and identifying genetic risks, chemoprevention and avoiding risk factors reduces the risk of developing breast cancer and helps reduce its morbidity and mortality, but this does not mean that you will not get cancer [15]. The increasing understanding of the mechanisms behind the development of breast cancer has allowed researchers to focus on the populations most likely to benefit. The development of safe and efficient agents, the use of technology, and the personalization of preventive treatments are all important for the growth and value of cancer prevention research [16].

In the last decades, many studies focusing on modulation of cancer progression have involved in three highly important enzyme families: (**i**) The phosphatidylinositol-3-kinases (PI3Ks)/AKT, also called phosphoinositide 3-kinases, which are a family of enzymes involved in cellular functions such as intracellular trafficking, cell growth, proliferation, differentiation, motility and survival that are in turn involved in cancer [17], (**ii**) the mammalian target of rapamycin (mTOR) that is a central regulator of cellular and organismal growth, homeostasis, and cellular metabolic processes, including macromolecular synthesis, ribosome biogenesis, and autophagy [17b,18], and (**iii**) histone deacetylases (HDACs), that are enzymes catalyzing removal of acetyl functions from the lysine residues of both histone and nonhistone proteins [19]. Inhibition of such enzymes are among the current treatment approaches for the effective treatment of breast cancer and the related brain metastases. The principles in such approaches are based on the direct targeting tumors and proteins with various expression levels by inhibiting the signaling pathways of such enzymes that play a highly important role on the progress of the breast cancer modulation [9]. In particular, inhibition of HDAC and mTOR enzymes has appeared to be a high potential strategy [20]. Numerous HDAC and mTOR inhibitors have been viewed as highly potent agents that have shown very significant anticancer activities in preclinical studies [20–26]. Another study [26] has demonstrated that mTOR has a crucial and important function in the PI3K/AKT signaling pathway, controlling

angiogenesis, cell growth, and survival, which becomes a main target for the development of novel anticancer treatments.

Due to the central roles of mTOR, PI3K/AKT and HDAC as a novel potent anticancer therapy approach [22–24], the targeted inhibition of these enzymes and controlling their signaling pathways are very essential to combat with the cancer cells. In particular, HDAC and mTOR inhibitions are very important potent and promising approaches as anticancer therapy. Due by the importance of these two enzymes, most researchers have, therefore, focused their research on developing novel inhibitors targeting mTOR and HDAC to determine the exact mechanism of action for mTOR and HDAC inhibition. For instance, Fasolo and Sessa [26] have studied on the development of mTOR inhibitors with various targets. In another study, the bio-assessment of dual mTOR/HDAC6 inhibitors against MDA-MB-231 cells for triple negative breast cancer (TNBC) treatment have been studied [20]. In this study, Yao and coworkers have created and designed a novel series of dual inhibitors via the structure-based strategy, synthesized such inhibitors, and discovered that one of the inhibitors had the potential to be a dual inhibitor with $IC_{50}$ value of 56 nM against HDAC6 and 133.7 nM against mTOR, which demonstrated significant antiproliferative action when applied in TNBC cells. In another study, suppressing invasion and proliferation of the breast cancer cells through miR-200c regulation targeting CRKL by an HDAC inhibitor has shown by Bian and coworkers [23]. In this inhibition process, they have observed that considerable downregulation of miR-200c in breast cancer cell lines as compared to normal cell lines, in which this downregulation and correlation suggest a significant diagnostic marker and a promising therapeutic target. Guo and coworkers have studied HDAC1 expression and retinoblastoma binding protein 4 by associating with clinicopathologic characteristics and prognosis and found that such expression was noticeably higher compared to normal tissues [22], claiming that HDAC1 controls the transcription/translation of the estrogen and progesterone receptors in this mechanism. The overexpression of HDAC1 that modulates progression in breast cancer has also been studied [25], and found the suppression and transcriptional activity due to the interaction of HDAC1 with the estrogen receptor α both *in vivo* and *in vitro,* strongly suggesting the effect of HDAC1 on the breast cancer progression. Thus, HDAC1 may be a therapeutic intervention potent for the treatment for an estrogen receptor-negative breast cancer subset. A novel and

promising strategy for the cancer therapy could be provided by inhibiting HDAC1 expression or activity. The roles of estrogen receptor α and mechanistic resistance to endocrine therapy have also been investigated by Lu and Liu [27]. In addition, they have reported the potent selective estrogen receptor degraders (SERDs) as a promising novel treatment methods for the breast cancer. Tang and coworkers [24] demonstrated that HDAC1-induced overexpression of interleukin-8 (IL-8) led to the migration and proliferation of breast cancer cells, where they found that mRNA and HDAC1 levels in 3/4 of the breast cancer cells are higher than the corresponding adjacent normal cells. From the data, they have claimed that inhibition of the IL-8 expression and the breast cancer cell proliferation and migration may be suppressed by the HDAC1 knockdown by specific siRNAs, which in turn suggests that HDAC1 might be a promising therapeutic target for the treatment of breast cancer. In another study, Min et al. [21] have examined antitumor activity of an HDAC inhibitor, namely IN-2001, and studied the molecular mechanisms effective on MDA-MB-231 (231) cells. In addition to the abovementioned literature studies, there have been many other novel potent anticancer agent studies [28] in the field for better recognition and comprehension of cellular and molecular mechanisms of both mTOR and HDAC inhibition.

The current literature [1–28] clearly states that several inhibitors have been designed, synthesized, and evaluated for their anticancer and antitumor activities, along with their mechanisms of action on breast cancer cells, and there is still an urgent demand for more of such novel artificial inhibitors for HDAC and mTOR enzymes and their signaling pathways in particular. A reliable and significant number of literature reports have highlighted the effective function of transition metal complexes as anticancer agents, as well as their promise anticancer chemotherapeutic potential [28a–c, 22]. Due by the inhibition of colorectal cancer progression [30], *in vitro* and *in vivo* use of potential anticancer and nonsteroidal anti-inflammatory therapeutics [31], copper homeostasis [29a,b,i], and use as anticancer [32] and antitumor [33,34] therapeutics, copper metal/ion plays very important role in mammalian cells. Regarding the complexes, 1,10-phenanthroline (PHEN) and its derivatives with transition metals (*e.g.*, copper(Cu)) have been widely used for the treatment of various cancer types, *e.g.*, breast cancers and brain metastasis following lung cancer [28d] due to planar structure of the PHEN, a metal chelator. Many metal complexes with PHEN and Schiff bases that have a C=N functional group play very important roles and possess anticancer

activity [35]. Such copper complexes are highly intriguing due to their diverse biological activities, antimycobacterial [28f], antimicrobial [28g], antitumor [28e], and intercalating agents of DNA [28h].

Cu metal/ion is a very important mineral nutrient and it is both toxic and beneficial to the cell due to its well-known oxidation states. It is gradually linked to both cell proliferation and pathways leading to death. Thus, it is a required host cofactor [29c,d]) of vital cellular functions for enzymes, *e.g.*, antioxidant defence, pigments, biosynthesis of hormones, neurotransmitters, and mitochondrial respiration. In addition, dysregulation of copper stores can also cause the induction of oxidative stress and cyctotoxicity [29e–h]. Denoyer, Ge and Li [29a,b,i] simultaneously have studied transition metal signaling that has created new connections between chemists and biologists, which in return benefits translating basic copper science into clinical therapies and diagnostics to further exploit the weaknesses in diseases linked to copper.

Copper and its coordination compounds have a very obvious fundamental regulation role in metastasis and they can be used as a single agent and in combination with others proved by many clinical and precilinical studies [29a], *e.g.*, successful treatments of brain, ovarian, bladder and breast cancers [28i–k]. In addition to the PHEN and its derivatives with a metal complexes, *e.g.*, copper, a known natural medicine Prodigiosin (Ps) [28l] is another structure as a secondary and natural metabolite, which has multiple biological functions, including but not limited to anti-inflammatory, antibacteria, immnosupression and anticancer activity [28m]. Ps has also attracted immense interests with its anticancer function because it is a dual mTOR inhibitor, which has two essential components (mTORC1 — survival and tumor cell proliferation and mTORC2 — invasion and cell migration [28n]) for the mTOR pathway, necessary for cancer development. A recent study [28o] has shown that Ps can block Wnt/β-catenin signaling pathway. Since this pathway plays a role in the development and spread of cancer, Ps may be a promising candidate for a next-generation anticancer drug due to its unique inhibition mechanisms, and its derivatives have also become one of the most promising anticancer drug classes leading with anticancer and proapoptotic effects in a variety of cancer cell lines including breast cancer cells in recent years [36] even though the structure was first ascertained from a total synthesis in 1960 [37]. The synthesis of Ps derivatives is receiving increased attention in current research because of their anticipated

lower cytotoxicity and anticancer efficacy. Another research area that is at least as important as mTORs is the inhibition of the HDAC because deregulation of Class I HDAC (HDAC1, 2, 3 and 8) activity has been associated with many cancer types [28p–s] and its involvement has been [28t] extremely critical in regulating mammalian cell proliferation. HDAC1 and its overexpression, in particular, have been related to various types of cancer [28u–w]. Thus, inhibition of HDAC1 becomes a potentially effective therapeutic target for cancer treatment, this may be controlling the progression of breast cancer and related metastasis [28w,x].

A major downside to commercially available common anticancer drugs (*e.g.*, fluorouracil, doxorubicin, carboplatin, and paclitaxel) on the market for the treatment of breast cancer is the buildup of resistance toward these drugs by cancer cells. Novel drugs with alternative modes of action are vital to ensure both the effectiveness and worldwide affordability of cancer treatments. As it currently stands, neither PHEN nor Ps or their any derivatives has made any commercial progress to the current anticancer drug market. Even though one of the candidate drugs, obatoclax, passed the phase II clinical trials, its development was unfortunately halted. Thus, alternative PHEN and Ps derivatives have yet to be tested as therapeutic agents for combatting breast cancer. In one of our earlier preliminary studies [38], some Ps and PHEN derivatives with their copper(I) complexes, were isolated, characterized, and their biological activities were also *in vitro* tested on six different cell lines. Some of the studied ligands and/or their relevant complexes exhibited promising anticancer activities against the highly interested cell line, 231BR. One of the ligands presented in the study showed an overwhelming anticancer activity than Ps, the natural drug. When compared ligands with their relevant copper(I) complexes, the complexes were even performed more significant anticancer activities on the selected cell lines. The *in silico* computational modeling studies carried out with mTOR and HDAC1 enzymes also validated the obtained experimental data.

In this context, the main goal of this study is to design and create novel PHEN and Ps derivatives as well as their copper(I) complexes as active pharmaceutical ingredients (APIs), which will inhibit HDAC (especially HDAC1) and/or mTOR enzymes against brain metastatic breast cancer. By utilizing the current literature [1–37] and the highly rewarding preliminary results from our earlier study [38], we, in this work, have focused on designing and optimizing novel PHEN and Ps derivatives by employing *in silico*

computational modeling studies that are carried out with mTOR and HDAC1 enzymes considering the *in silico* structure-activity relationship (*in silico* SAR). Such structural and modeling studies have facilitated to predict the most promising functions/functional groups with the PHEN and Ps core structures (**Figure 1.1**), binding affinities and binding modes of such desired ligands. Some of these ligands have structurally been modified and optimized to direct our synthetic routes to obtain such novel PHEN and Ps derivatives as well as their copper(I) complexes. With the preliminary results, we predict that either PHEN and/or Ps derivatives including their copper(I) complexes or the combined use of such compounds in different variations, given their numerous modes of cellular actions, could improve the efficacy of anti-cancer treatments and offer significant therapeutic potential for the breast cancer patients with brain metastasis risk.

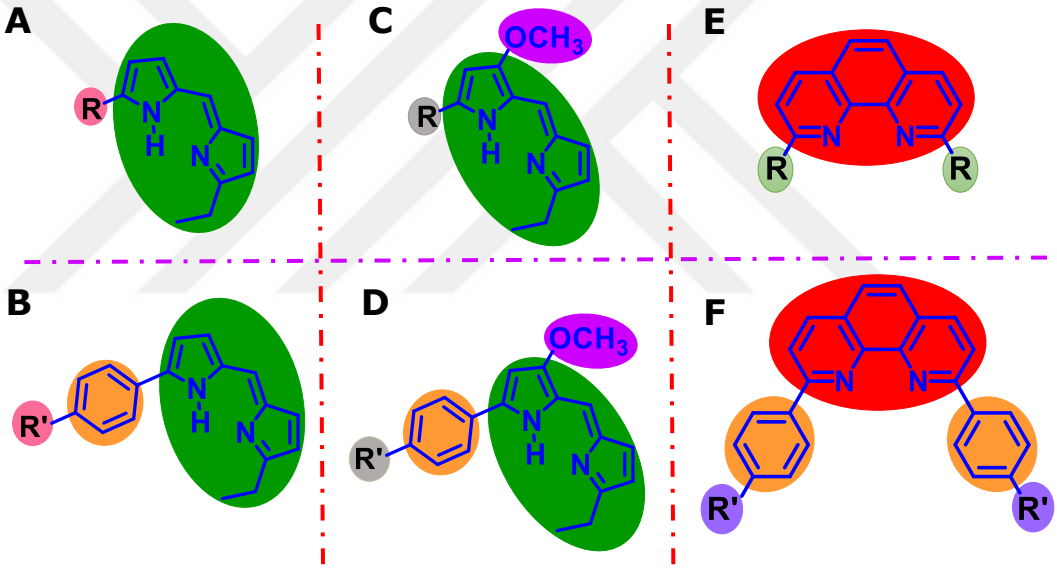


**Figure 0.1** The general structures of Ps- (**A, B, C** and **D**) and PHEN (**E** and **F**)-based derivatives and their functionalization with different **–R, –R'** and/or –**phenyl-R'** groups.

# 2. MATERIALS AND METHODS

By aiming to structurally design and develop novel PHEN and Ps derivatives, some *in silico* computational modeling studies that have been carried out with mTOR and HDAC1 enzymes considering the *in silico* SAR details are presented below.

## 2.1 Molecular Modeling Studies

### 2.1.1 Enzyme preparation

The mTOR and HDAC1 crystal structures were retrieved from protein data bank and used for the protein setup. [(http://www.rcsb.org, (for mTOR pdb code: 4jsv; resolution 3.5 Å) and (for HDAC1, pdb code: 4BKX; resolution 3.0 Å)] [39]. Each structure was cleaned of all water molecules and inhibitors as well as all non-interacting ions before being used in the docking studies. One of the two subunits for mTOR and HDAC1 was chosen as the target structure. Each protein's geometry was first optimized using a fast Dreiding-like force field, and subsequently submitted to Discovery Studio's "Clean Geometry" toolset [40] for a more thorough examination. Missing hydrogen atoms were added considering the protonation state of the titratable residues at a pH of 7.4. The dielectric constant was adjusted to 10 and the ionic strength was set to 0.145. The AutoDock Tools (vv. 1.5.7) (ADT) [41] graphical user interface program was employed to setup the enzymes for docking.

### 2.1.2 Ligand setup

The three-dimensional (3D) structures of ligand molecules were built and minimized using BIOVIA Discovery Studio [40], and optimized at (PM3) level and saved in pdb format. Here, the docking input files of the ligands were also generated using the ADT package. Autodock Vina [43] docking program was used for all docking processes. In an

earlier literature work [42], the comprehensive procedure used for docking methods was explained in detail.

### 2.1.3 Molecular docking

The data constructed with the BIOVIA Discovery Studio [40] was saved in pdb format, and in the meantime, missing hydrogen atoms were added considering the protonation state of the titratable residues at a pH of 7.4, also optimization of geometry and minimization processes were employed. Upon preparation of the ligands, molecular docking was performed using the Autodock Vina [43] with the parameters in **Table 2.1**.

**Table 2.1** The molecular docking grid center and box dimensions used for Autodock Vina.

| Center (Å) | HDAC1 | mTOR | Box Dimensions (Å) | HDAC1 | mTOR |
|---|---|---|---|---|---|
| **X** | -46.7 | -20.7 | **X** | 25 | 25 |
| **Y** | 16.3 | -29.9 | **Y** | 25 | 25 |
| **Z** | -7.8 | -58.3 | **Z** | 25 | 25 |

### 2.1.4 Molecular dynamic simulations

Of the designed and optimized 75 ligands (**Figures 2.1–2.3**), six enzyme-ligand complexes (**2a**, **6b** and **13** against the HDAC1 and **6b**, **13** and **13a** against the mTOR) have produced the best results for each virtual screening technique chosen based on their binding energies in order to investigate the structural dynamics and stability of these complexes (**Tables 3.1–3.3**). Using the BIOVIA Discovery Studio [40], the six selected enzyme-ligand complexes and the free HDAC1 and mTOR enzymes were prepared [44] for NAMD input file processing. The input files for NAMD were prepared using Charmm-GUI [45] that was employed for each enzyme-ligand complex and free HDAC1 and mTOR enzymes. NAMD was used to run unconstrained 50 nanosecond (ns) Molecular Dynamics (MD) simulations on both free enzymes and enzyme-ligand complexes. The validation of the complexes with the free enzymes was examined by comparing the average values of root-mean-square deviations (RMSD), root-mean-

square fluctuation (RMSF), radius of gyration (Rg) profiles along the trajectories on the generated graphs.

## 2.2 Chemistry

### 2.2.1 Design of Ps-based, Ps and PHEN derivatives as novel ligands

One of the most important studies that needs to be accomplished is to create and design chemical structures that will first exhibit highly promising *in silico* computational modeling results, and then the synthetic possibility with potential anticancer activities. Because not every drug candidate performing anticancer activity can synthetically be obtained, or *vice versa*. Therefore, considering our previous experiences and results from the highly promising preliminary study [38] regarding validation of the computational data for the designed chemical structures and their biological activities with some Ps and PHEN ligands as well as their relevant complexes with HDAC1 and mTOR enzymes, it has been aimed to carry out further studies to create, design and develop novel improved and optimized Ps-based and Ps (**Figures 2.1** and **2.2**), and PHEN (**Figure 2.3**) derivatives by even further enabling the synthesis, isolation, characterization, and *in vitro* biological activity testing of such novel compounds that have never been studied beforehand. In this regard, first a series of Ps-based derivatives have been designed in order to evaluate the absence of the methoxy group (–$OCH_3$) and effect of the –phenyl group (–Ph) on one of the pyrrole rings (**1–13** (presence of –Ph, but absence of –$OCH_3$) and **14–26** (absence of both –Ph and –$OCH_3$) in the **Figure 2.1**).

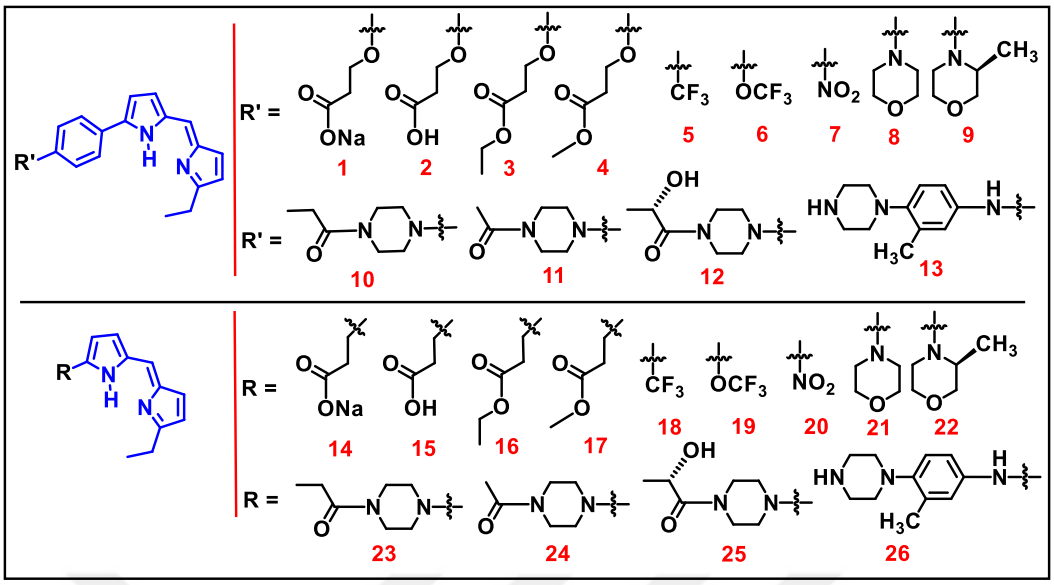


**Figure 2.1** The Ps-based derivatives with various functions introduced into the structure for determining relationships between chemical structures and *in silico* biological activity (*in silico* SAR) of the designed compounds.

Based on the outcomes of the Ps-based derivatives (**Table 3.1**), a series of Ps derivatives have further been designed and evaluated in the presence and absence of the –Ph group on the same pyrrole ring that has the –$OCH_3$ group (**Figure 2.2**). The obtained results (**Tables 3.1** and **3.2**) and discussion of both sets of derivatives are presented in the **Results and Discussion Section**.

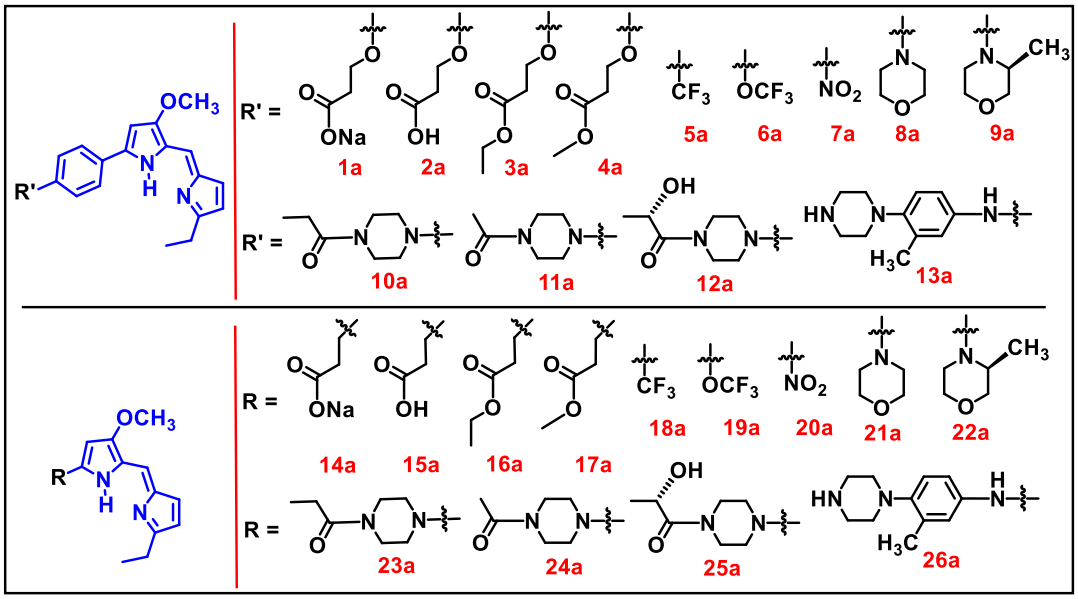


**Figure 2.2** The Ps derivatives with various functions introduced into the structure for determining relationships between chemical structures and *in silico* biological activity (*in silico* SAR) of the designed compounds.

Upon completion of both Ps-based (**1–26**) and Ps derivatives (**1a–26a**), the PHEN structure has been used to replace the Ps-core structure, conducted similar *in silico* computational modeling studies for a series of PHEN derivatives (**Figure 2.3**) and obtained results for both binding energies and inhibition constants of such compounds (**Table 3.3**).

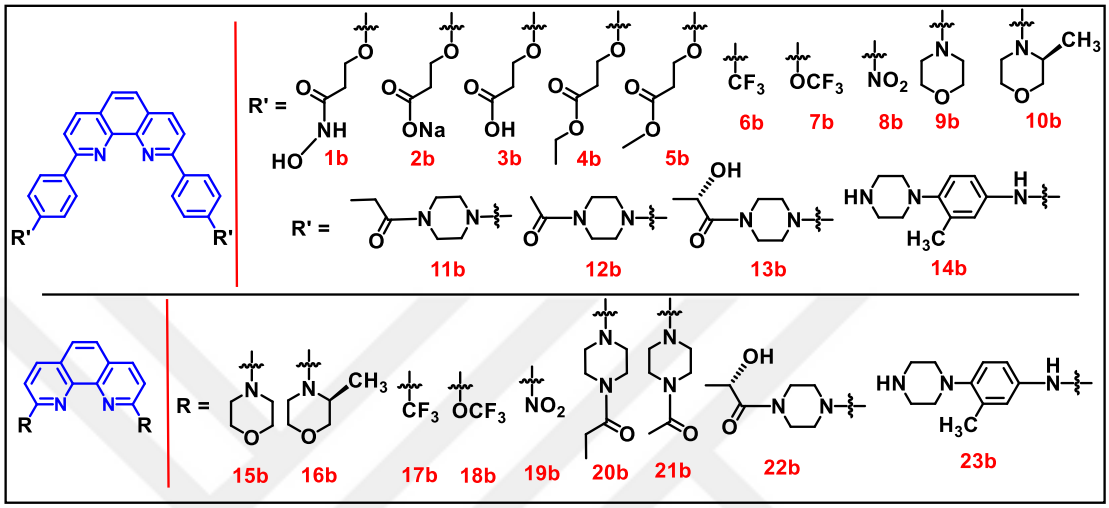


**Figure 2.3** The PHEN-based derivatives with various functions introduced into the structure for determining relationships between chemical structures and *in silico* biological activity (*in silico* SAR) of the designed compounds.

# 3. RESULTS AND DISCUSSION

Since not every novel and computationally highly potent and effective therapeutic drug or API candidate showing anticancer activity can be obtained synthetically or most synthetically accessible candidates may not have any anticancer activity, reviewing the literature for the possibility of both synthetic accessibility and anticancer activity is one of the most crucial studies. In the light of this information, a series of Ps-based, Ps and PHEN derivatives (75 derivatives in total, **Figures 2.1–2.3**) as therapeutic drug or API candidates have been designed and optimized using *in silico* computational modeling studies. More importantly, some of these derivatives/ligands have exhibited very promising binding energies and inhibition constants (**Tables 3.1–3.3**) against HDAC1 and/or mTOR enzymes (**Figure 3.1**) after forming enzyme-ligand complexes.

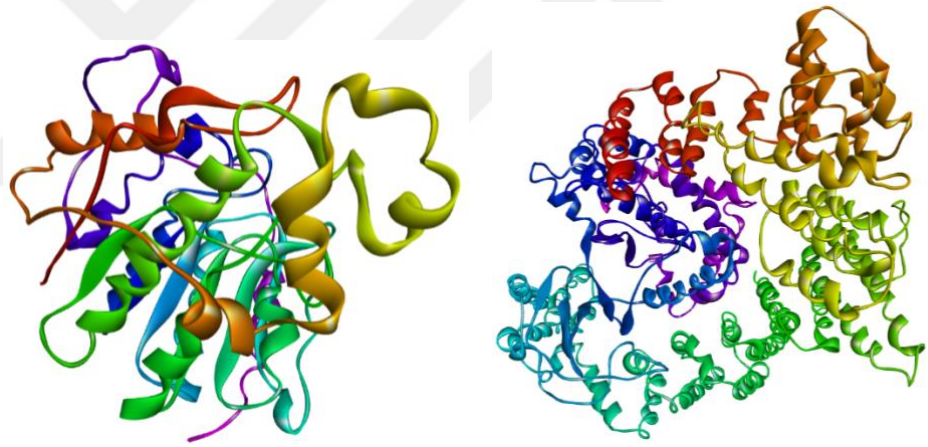

**Figure 3.1** The structural representation of free HDAC1 (left) and mTOR (right) enzymes.

As in general practice for being highly effective, a time-efficient tool of *in silico* computational modeling has initially been utilized to collect initial results for the designed 75 ligands from the docking studies into the active sites of HDAC1 and mTOR enzymes to predict their binding affinities and binding modes by employing the AutoDock Vina docking software [43]. Since acquiring the Molecular Dynamics (MD) simulations for each ligand would relatively require longer time intervals, selecting some of the ligands with the best binding energies and inhibition constants have been targeted for the MD simulations after collecting the initial results. Of these 75 ligands, 20 of them (**1**, **1a**, **1b**,

**2**, **2a**, **2b**, **3**, **3b**, **5**, **5a**, **6b**, **7**, **7a**, **7b**, **8b**, **12b**, **13**, **13a**, **14b** and **23b**), which are highly potent to inhibit HDAC (especially HDAC1) and/or mTOR enzymes against brain metastatic breast cancer, have exhibited very promising binding energies and inhibition constants (**Tables 3.1–3.3**) against at least one or both enzymes, but preferentially both.

**Table 3.1** Calculated binding energies (in kcal/mol) and inhibition constants (in nM) for Ps [38] and Ps-based derivatives (**Figure 2.1**) against the mTOR and HDAC1 enzymes.

| Compound ID | mTOR | | HDAC1 | |
|---|---|---|---|---|
| | **Binding Energies (kcal/mol)** | **Inhibition Constants (nM)** | **Binding Energies (kcal/mol)** | **Inhibition Constants (nM)** |
| **Ps*** | -4.89 | 258.68 μM | -6.99 | 7.53 μM |
| **1** | -7.1 | 547 | -8.4 | 336 |
| **2** | -7.2 | 547 | -8.6 | 310 |
| **3** | -6.6 | 697 | -8.1 | 380 |
| **4** | -6.9 | 617 | -8.1 | 380 |
| **5** | -8.1 | 380 | -8.5 | 323 |
| **6** | -7.4 | 505 | -8.0 | 396 |
| **7** | -8.0 | 396 | -8.1 | 380 |
| **8** | -7.3 | 525 | -7.7 | 447 |
| **9** | -7.4 | 505 | -7.7 | 447 |
| **10** | -7.4 | 505 | -7.3 | 525 |
| **11** | -7.4 | 505 | -7.7 | 447 |
| **12** | -7.6 | 465 | -7.7 | 447 |
| **13** | -8.2 | 365 | -8.5 | 324 |
| **14** | -6.3 | 786 | -7.1 | 569 |
| **15** | -6.5 | 726 | -7.1 | 569 |
| **16** | -6.1 | 853 | -7.1 | 569 |
| **17** | -6.3 | 786 | -7.0 | 593 |
| **18** | -6.4 | 755 | -7.3 | 525 |
| **19** | -6.6 | 697 | -7.5 | 485 |
| **20** | -6.2 | 819 | -7.4 | 505 |
| **21** | -6.7 | 669 | -7.4 | 505 |
| **22** | -7.1 | 547 | -6.9 | 617 |
| **23** | -7.0 | 593 | -7.4 | 505 |
| **24** | -7.1 | 547 | -7.4 | 505 |
| **25** | -6.8 | 643 | -7.1 | 569 |
| **26** | -7.4 | 505 | -7.5 | 485 |

***This data was taken from the previous study [38] for the comparison purpose only.

**Table 3.2** Calculated binding energies (in kcal/mol) and inhibition constants (in nM) for Ps [38] and Ps derivatives (**Figure 2.2**) against the mTOR and HDAC1 enzymes.

| Compound ID | mTOR | | HDAC1 | |
|---|---|---|---|---|
| | **Binding Energies (kcal/mol)** | **Inhibition Constants (nM)** | **Binding Energies (kcal/mol)** | **Inhibition Constants (nM)** |
| **Ps*** | -4.89 | 258.68 μM | -6.99 | 7.53 μM |
| **1a** | -7.2 | 547 | -8.4 | 337 |
| **2a** | -7.1 | 569 | -8.5 | 324 |
| **3a** | -6.8 | 643 | -8.0 | 396 |
| **4a** | -6.7 | 669 | -8.1 | 380 |
| **5a** | -7.9 | 412 | -8.2 | 365 |
| **6a** | -7.4 | 505 | -7.5 | 485 |
| **7a** | -7.7 | 447 | -7.9 | 412 |
| **8a** | -7.0 | 593 | -7.5 | 485 |
| **9a** | -7.1 | 569 | -7.9 | 412 |
| **10a** | -7.2 | 547 | -7.3 | 525 |
| **11a** | -7.3 | 525 | -7.6 | 465 |
| **12a** | -7.6 | 465 | -7.7 | 447 |
| **13a** | -8.3 | 351 | -8.3 | 351 |
| **14a** | -6.4 | 755 | -6.8 | 643 |
| **15a** | -6.7 | 669 | -6.8 | 643 |
| **16a** | -6.1 | 853 | -6.6 | 697 |
| **17a** | -6.4 | 755 | -6.7 | 669 |
| **18a** | -6.4 | 755 | -6.7 | 669 |
| **19a** | -6.2 | 819 | -6.6 | 697 |
| **20a** | -6.2 | 819 | -6.2 | 819 |
| **21a** | -6.5 | 726 | -6.7 | 669 |
| **22a** | -6.9 | 617 | -6.7 | 669 |
| **23a** | -6.6 | 697 | -7.3 | 525 |
| **24a** | -6.7 | 669 | -7.3 | 525 |
| **25a** | -6.7 | 669 | -7.0 | 593 |
| **26a** | -7.1 | 570 | -7.3 | 525 |

*****This data was taken from the previous study [38] for the comparison purpose only.

**Table 3.3** Calculated binding energies (in kcal/mol) and inhibition constants (in nM) for Ps [38] and PHEN derivatives (**Figure 2.3**) against the mTOR and HDAC1 enzymes.

| Compound ID | mTOR | | HDAC1 | |
|---|---|---|---|---|
| | **Binding Energies (kcal/mol)** | **Inhibition Constants (nM)** | **Binding Energies (kcal/mol)** | **Inhibition Constants (nM)** |
| **Ps*** | -4.89 | 258.68 μM | -6.99 | 7.53 μM |
| **1b** | -7.2 | 547 | -9.1 | 254 |
| **2b** | -7.9 | 412 | -8.7 | 299 |
| **3b** | -8.1 | 380 | -9.1 | 254 |
| **4b** | -7.2 | 547 | -7.8 | 429 |
| **5b** | -7.3 | 525 | -8.6 | 311 |
| **6b** | -9.4 | 225 | -9.4 | 225 |
| **7b** | -9.0 | 264 | -9.4 | 225 |
| **8b** | -8.9 | 275 | -8.5 | 324 |
| **9b** | -8.0 | 396 | -8.4 | 337 |
| **10b** | -8.3 | 351 | -7.3 | 525 |
| **11b** | -8.3 | 351 | -8.6 | 311 |
| **12b** | -8.9 | 275 | -8.7 | 299 |
| **13b** | -8.7 | 299 | -6.9 | 617 |
| **14b** | -9.2 | 244 | -8.7 | 299 |
| **15b** | -6.6 | 697 | -6.8 | 643 |
| **16b** | -7.1 | 569 | -7.3 | 525 |
| **17b** | -7.7 | 447 | -8.5 | 324 |
| **18b** | -7.3 | 525 | -8.5 | 324 |
| **19b** | -6.9 | 617 | -7.5 | 485 |
| **20b** | -7.1 | 569 | -6.7 | 669 |
| **21b** | -7.2 | 547 | -6.7 | 669 |
| **22b** | -7.6 | 465 | -7.1 | 569 |
| **23b** | -8.9 | 275 | -7.8 | 429 |

***This data was taken from the previous study [38] for the comparison purpose only.

As shown in the **Tables 3.1–3.3**, the data taken from our previous study [38] presents that the natural product Ps exhibits –4.89 kcal/mol binding affinity and 258.68 μM inhibition constant against mTOR while having –6.99 kcal/mol and 7.53 μM against HDAC1, respectively. Compared to the novel ligands, Ps definitely has lower binding affinity and inhibition constant for the most cases against either one or both enzymes. Among these 75 ligands, **1**, **1a**, **1b**, **2**, **2a**, **2b**, **3**, **3b**, **5**, **5a**, **6b**, **7**, **7a**, **7b**, **8b**, **12b**, **13**, **13a**, **14b**, and **23b** have exhibited highly promising binding energies and inhibition constants (**Tables 3.1–3.3**) against at least one or both enzymes. While Ps-based ligands **5**, **7** and **13** on mTOR

(average of –8.1 kcal/mol and 380 nM) and **1**, **2**, **5**, and **13** (average of –8.5 kcal/mol and 323 nM) on HDAC1 have exhibited very promising results on at least one of the enzymes, ligands **5** (–8.1 kcal/mol and 380 nM against mTOR and –8.5 kcal/mol and 323 nM against HDAC1) and **13** (–8.2 kcal/mol and 365 nM against mTOR and –8.5 kcal/mol and 324 nM against HDAC1) in particular have showed very effective results (**Table 3.1**) with dual action against both enzymes. In the case of Ps derivatives, ligands **1a**, **2a**, **5a**, **7a** and **13a** have exhibited higher binding affinities and inhibition constants (average of –7.6 kcal/mol and 465 nM against mTOR, and average of –8.2 kcal/mol and 371 nM against HDAC1, respectively) against at least one or both enzymes, where ligands **5a** and **13a** have been highly effective on mTOR and **1a**, **2a** and **5a** on HDAC1. However, the ligand **5a** (–7.9 kcal/mol and 412 nM against mTOR and –8.2 kcal/mol and 365 nM against HDAC1) has particularly showed promising binding energy and inhibition constant values (**Table 3**) with dual action against both enzymes. In these two sets of data (**Tables 3.1** and **3.2**), the results have showed that presence and absence of the –Ph group on the pyrrole ring without $–OCH_3$ group (**Figure 2.1**) have affected the binding affinity and binding mode of the ligands within the same set of structures. Furthermore, existing of the $–OCH_3$ group on the same pyrrole ring (**Figure 2.2**) in the second set of structures (derivatives of the natural product Ps), simultaneous effectiveness of the ligands against both enzymes have changed regarding the binding energy and inhibition constant values (**Table 3.2**).

Upon completion of the *in silico* computational modeling (**Tables 3.2** and **3.3**) for the two sets of ligands in the **Figures 2.1** and **2.2**, the core structure of the Ps (**Figures 1.1C** and **1.1D** with $–OCH_3$ group) has been replaced with the PHEN core structure (**Figures 1.1E** and **1.1F**) in order to evaluate and compare the effect of the Ps-core and PHEN-core against both mTOR and HDAC1 enzymes. In the case of PHEN derivatives (**Figure 2.3**), ligands **1b**, **2b**, **3b**, **6b**, **7b**, **8b**, **12b**, **14b** and **23b** have exhibited higher binding affinities and inhibition constants against at least one or both enzymes (average of –8.6 kcal/mol and 322 nM against mTOR, and average of –8.8 kcal/mol and 390 nM against HDAC1, respectively), of which ligands **6b**, **7b**, **8b**, **12b**, **14b** and **23b** have been highly effective on mTOR and **1b**, **2b**, **3b**, **6b**, **7b**, **12b** and **14b** on HDAC1, respectively. The ligands **6b**, **7b**, **12b** and **14b** have showed highly promising binding affinities and inhibition constant values (**Table 3.3**) with dual action against both enzymes. Comparing with the Ps-based

and Ps derivatives, more number of PHEN derivatives have been exhibiting dual action against both enzymes (4 ligands) than the other two sets of structures (2 ligands in Ps-based and 1 ligand in Ps derivatives).

Our elaborated data from the *in silico* computational modeling studies has directed us to select the top dual-acting candidates with the best binding energy and inhibition constant from the **Tables 3.1–3.3** for further MD simulations that relatively require longer time intervals. Thus, ligands **5**, **5a**, **6b**, **7**, **13** and **13a** against mTOR and **1**, **1b**, **2a**, **6b**, **7b** and **13** against HDAC1 have been selected for the MD simulations. Among these ligands, five of them, **5**, **5a**, **6b**, **7b** and **13**, are highly important because they are the ones exhibiting dual action (the other dual-acting ligands **12b**, **13a** and **14b** were not utilized for MD simulations due to their lower binding energies and/or inhibition constants relative to the other five dual-acting ligands) against both mTOR and HDAC1 enzymes. From the **Tables 3.1–3.3**, the ligands **2a**, **6b** and **13** against HDAC1 and **6b**, **13** and **13a** against mTOR have found to be exhibiting the best results regarding the binding energies and inhibition constants compared to the other ligands. Ligand **6b** in particular shows relatively great binding affinity ($\Delta G$ = –9.4 kcal/mol and $K_i$ = 225 nM) against both HDAC1 and mTOR enzymes. On the other hand, ligands **2a** and **13** have exhibited relatively higher values for binding energies and inhibition constants ($\Delta G$ = –8.5 kcal/mol and $K_i$ = 324 nM) against HDAC1 while ligands **13** and **13a** have showed very similar results ($\Delta G$ = –8.2 kcal/mol and $K_i$ = 365 nM and $\Delta G$ = –8.3 kcal/mol and $K_i$ = 351 nM, respectively) against mTOR. Among these 4 ligands, **6b** and **13** are highly important due to their dual-acting capacity against both enzymes.

The poses of ligand **6b** in the binding pockets of HDAC1 and mTOR enzymes are presented in the **Figure 3.2** (**B** and **E** for two-dimensional (2D) and 3D images, respectively) and **Figure 3.3** (**A** and **B** for 2D and 3D images, respectively) , where two strong hydrogen bonds occur between ligand **6b** and the relevant amino acids (TYR303 and HIS28 amino acids against HDAC1 and the ARG2251 and VAL2240 against mTOR), in which both cases suggest the best inhibition of the enzymes (dual action) with ligand **6b** (potent dual inhibition candidate) among all other ligands. Relative to the ligand **6b**, ligands **2a** and **13** are the other two exhibiting great affinity against HDAC1 (**Figures 3.2A** and **3.2C** for 2D and **Figures 3.2D** and **3.2F** for 3D images, respectively). In the HDAC1–ligand **13** complex, there are three π-π stacked interactions with the PHE205,

HIS178 and PHE150 amino acids (**Figure 3.2C**) while the HDAC1–ligand **2a** complex exhibits two strong hydrogen bonds occurring between the ligand and the ASP176, TYR303 amino acids (**Figure 3.2A**). Such strong interactions support that these two ligands **2a** and **13** (second potent dual inhibition candidate) after ligand **6b** can act as highly promising other inhibitors against HDAC1 enzyme.

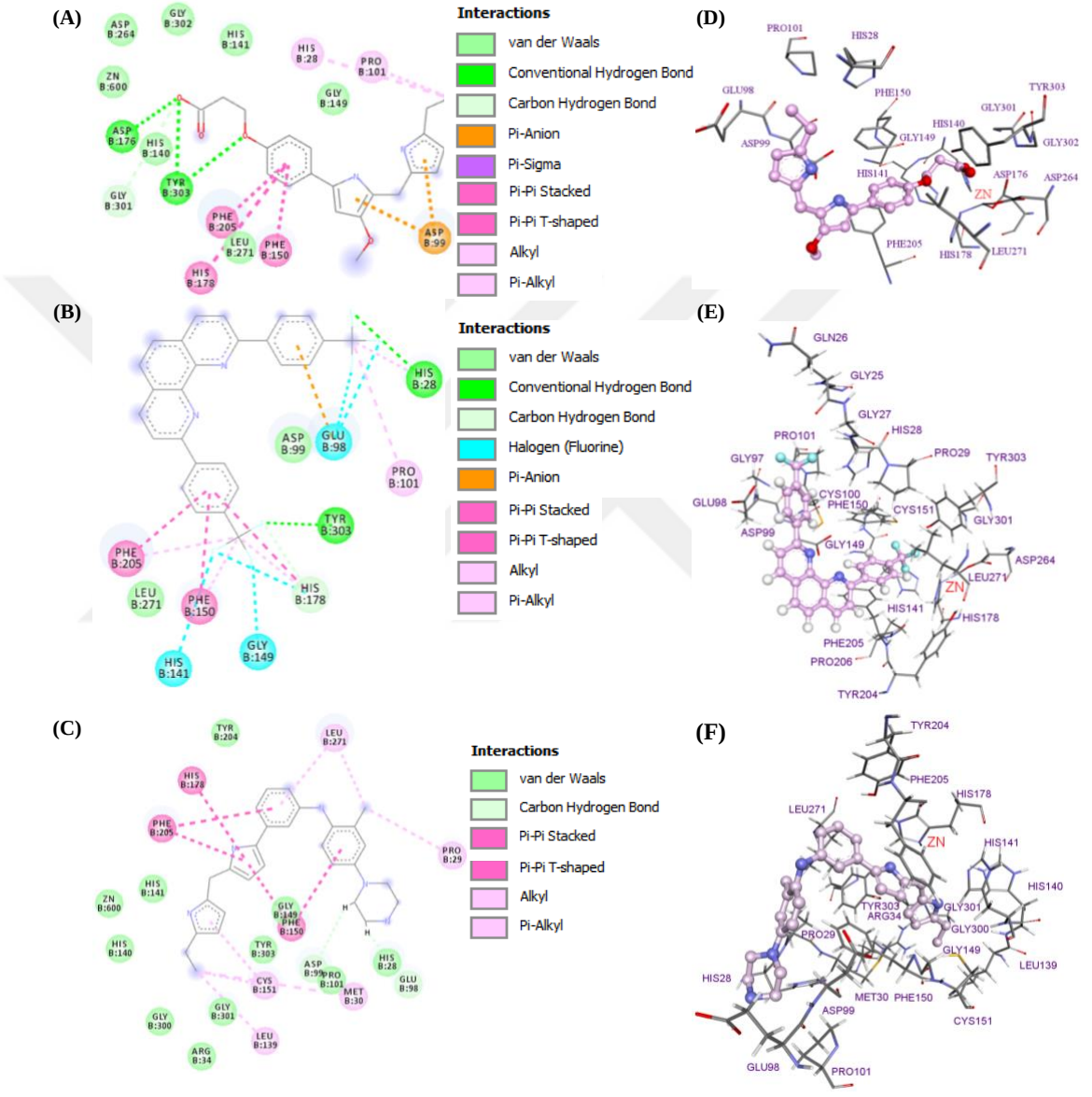


**Figure 3.2** The 2D **(A, B** and **C**) and 3D (**D, E** and **F**) images generated via molecular docking of the ligands **2a** (**A** and **D**), **6b** (**B** and **E**), and **13** (**C** and **F**) with the HDAC1 enzyme. Amino acid side chains are shown as sticks and the ligands as ball and sticks in 3D images.

The ligand **13** is also effective against the mTOR enzyme. In the mTOR–ligand **13** complex (**Figures 3.3B** and **3.3E**), there is a strong hydrogen bonding as well as π-π stacking between the ligand and the amino acids the THR2245 and TRP2239,

respectively. The ligand **13a** also exhibits great binding affinity against the mTOR enzyme (**Figures 3.3C** and **3.3F**), and there is a π-π T-shaped interaction between the ligand and TRP2239 amino acid upon formation of the complex. Although noncovalent interactions like π-π T-shaped are not as strong as hydrogen bonding, such interactions also play an important role in stabilizing molecular structures [46].

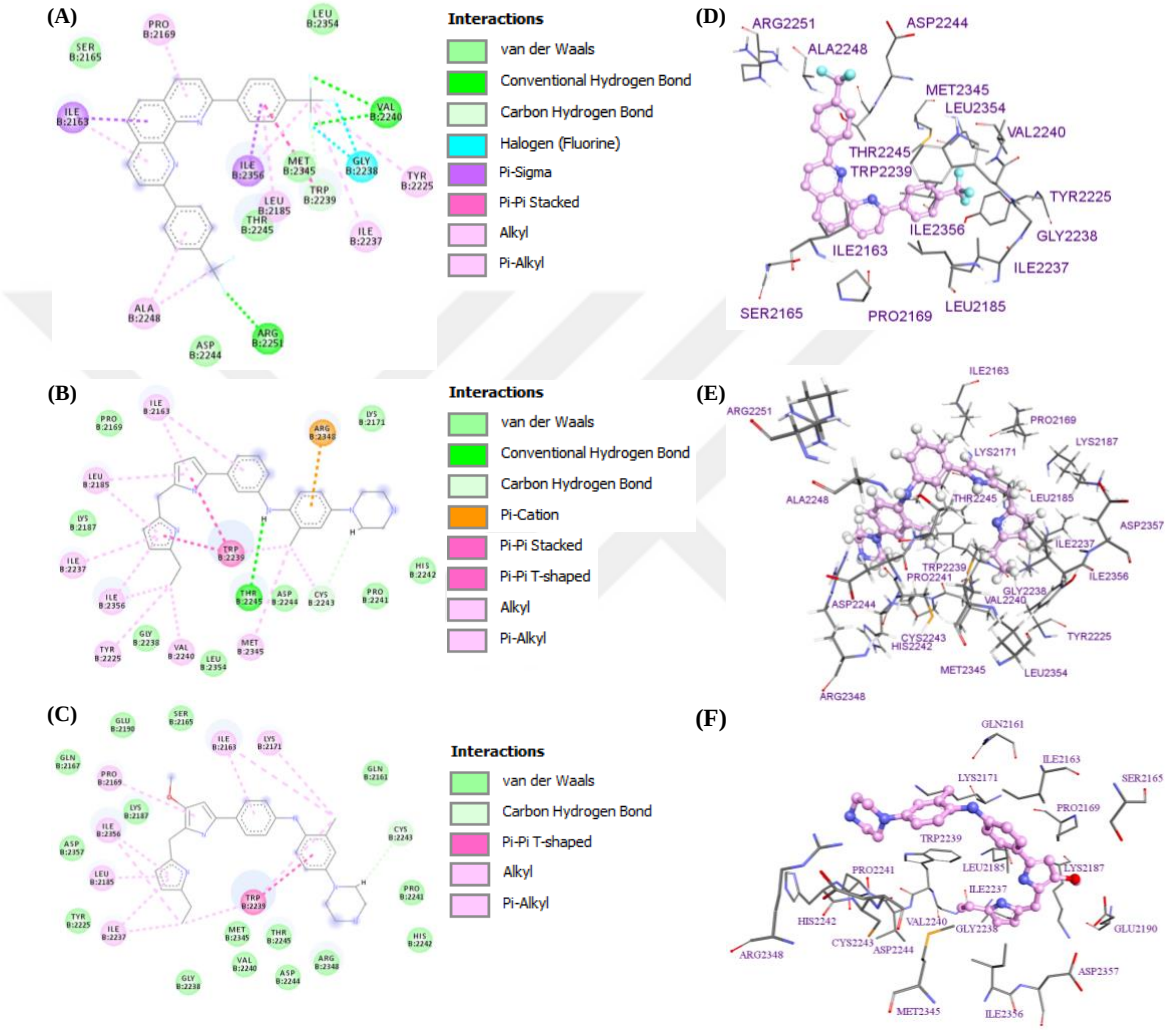


**Figure 3.3** The 2D (**A, B** and **C**) and 3D (**D, E** and **F**) images generated via molecular docking of the ligands **6b** (**A** and **D**), **13** (**B** and **E**), and **13a** (**C** and **F**) with the mTOR enzyme. Amino acid side chains are shown as sticks and the ligands as ball and sticks in 3D images.

Further investigation for various parameters such as, root-mean-square deviations (RMSD) for structural conformations and stability of enzymes upon complex formation, root-mean-square fluctuation (RMSF) for the flexibility/fluctuation of the complex, and radius of gyration (Rg) for the changes in the complex structures and information about overall dimensions (*i.e.*, consistent stability throughout the simulation), MD simulations for both free enzymes and enzyme-ligand complexes with the selected ligands have been

conducted, and the parameters have been calculated from the trajectory of MD simulations. The MD simulations of the ligands **2a**, **6b** and **13** against the HDAC1 and **6b**, **13** and **13a** against the mTOR enzymes have also provided highly supporting evidence for the abovefindings.

The combined RMSDs of both the complexes formed by binding of the ligands to free enzymes obtained through MD simulations are presented in **Figures 3.4** and **3.5** that provide average RMSD values of 1.74 and 3.47 Å (average RMSD for only globular proteins is less than 3 Å [47]) for free HDAC1 and mTOR enzymes, respectively. The average RMSDs of the HDAC1–ligand **6b** and mTOR–ligand **6b** complexes are of 2.14 and 3.92 Å (in green, **Figures 3.4** and **3.5**), respectively, and such higher values compared to the free enzymes suggest the presence of high degree of rotatable bonds or structural flexibilities that cause the ligand **6b** to be unable to attain stability inside the binding pocket of the enzymes in each case, which is assumed to be shallow. The average RMSD values of the the HDAC1–ligand **2a** and HDAC1–ligand **13** complexes are of of 2.09 and 2.20 Å (in blue and red, **Figure 3.4**), respectively, which are also higher than the RMSD value of the free HDAC1 enzyme. For such large complexes, the obtained values may be more acceptable compared to some simple structures. On the other hand, the average RMSD values of the the mTOR–ligand **13** and mTOR–ligand **13a** complexes are of 4.13 and 3.42 Å (in blue and red, **Figure 3.5**), respectively. While the RMSD value for the mTOR–ligand **13** complex is higher than the free mTOR enzyme, this value is found to be smaller in the case of mTOR–ligand **13a** complex.

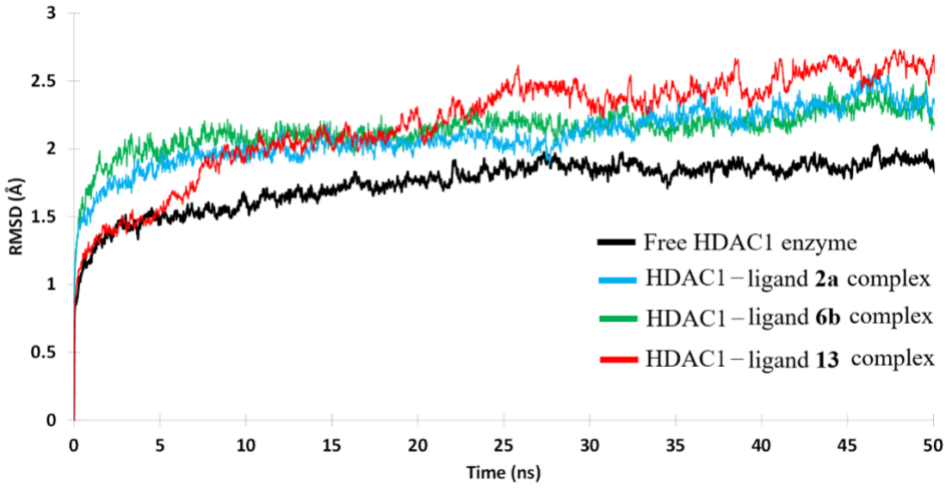


**Figure 3.4** The combined RMSD profiles from 50ns-MD simulations of both free HDAC1 enzyme (in black) and the complexes formed by binding of the ligands **2a** (in blue), **6b** (in green) and **13** (in red) to HDAC1.

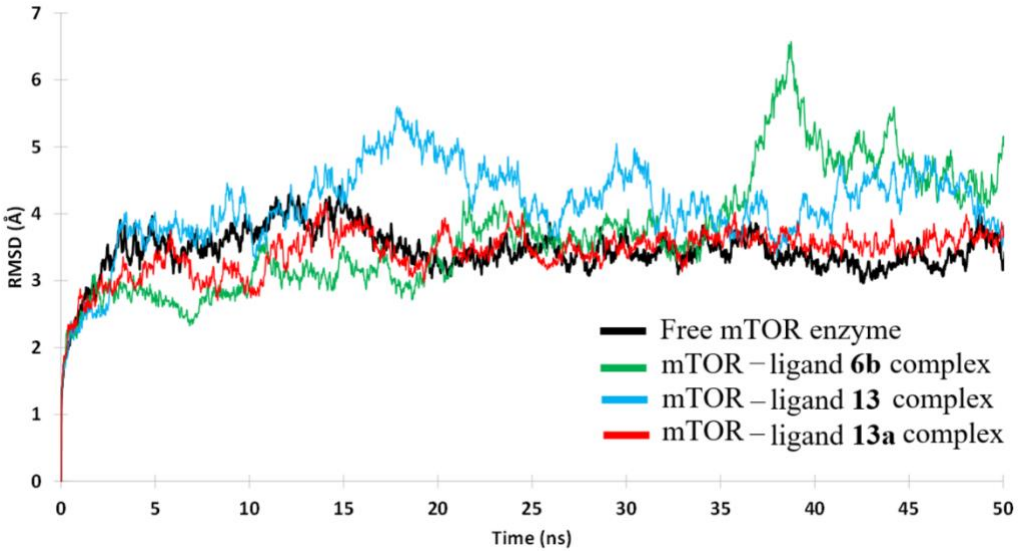


**Figure 3.5** The combined RMSD profiles from 50ns-MD simulations of both free mTOR enzyme (in black) and the complexes formed by binding of the ligands **6b** (in green), **13** (in blue) and **13a** (in red) to mTOR.

To better understand the deviation of amino acid residues of each complex relative to the reference position, the RMSFs, to which binding energies, ligand binding poses, and interactions entirely depend on [48], have been generated through the MD simulations (**Figures 3.6** and **3.7**), and collected and evaluated the information regarding the flexibility and dynamics of the complexes and individual fraction of each complex fluctuating from its mean structure (the ratio of fluctuation in the residual level). From the data, the average RMSF value (in black, **Figure 3.6**) for the free HDAC1 enzyme is of 0.76 Å. In the case of the HDAC1–ligand **6b** complex, the average RMSF value has been found to be 0.78 Å (in green, **Figures 3.6**). The result for the HDAC1–ligand **6b** complex can be interpretated in the manner of higher level of fluctuation, at which the residues 19, 78 and 91 in the complex produces higher RMSF values than the free enzyme whereas the case is opposite in the residues 201 and 368 of the free enzyme compared to the complex. Therefore, the complex has shown higher fluctuation pattern than the free ligand supported by the greater RMSF values, which indicate that the residues are located in the loop regions with more conformational flexibility. The RMSF values for the other complexes (0.75 Å and 1.00 Å for HDAC1–ligand **2a** and HDAC1–ligand **13**, respectively) have been obtained (in blue and red, **Figure 3.6**), and it is clearly evident that the residues 0, 19, 77, 198, and 261 from the HDAC1–ligand **13** complex have very sharp peaks while the free enzyme only has residue 368 exhibiting greater intensity. Thus,

this is confirming the higher fluctuation pattern for the complex as well. For the HDAC1–ligand **2a** complex, however, only residue 201 gives sharp peak for the complex while residue 368 does for the free enzyme. In the case of the RMSF values for the complexes of the ligands with the mTOR enzyme, the mTOR–ligand **6b** complex has an average RMSF value of 1.73 Å (in green, **Figure 3.7**) while the free mTOR enzyme exhibits 1.61 Å (in black, **Figure 3.7**). Similar results and predictions can be speculated for the complexes mTOR–ligand **13** (1.82 Å) and mTOR–ligand **13a** (1.84 Å) as well. The results also support that the free mTOR enzyme has shown lower fluctuation pattern than the complexes demonstrating that the restricted movements during the simulation. Thus, the residues located in the loop regions in the complexes have greater RMSF values that are corresponding to higher level fluctuations and more conformational flexibility rather than more constrained dynamics [49].

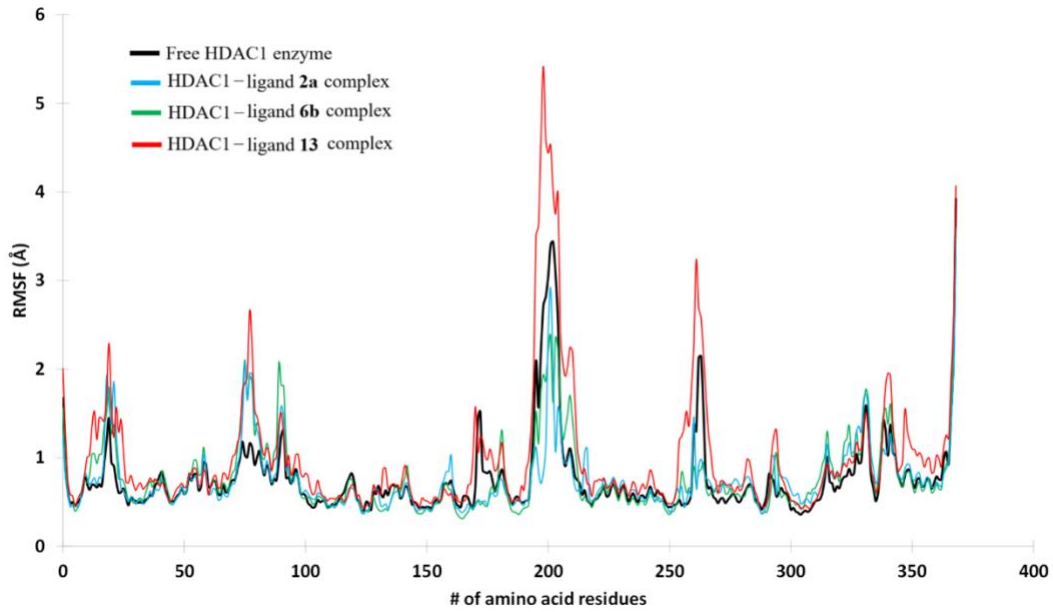


**Figure 3.6** The combined RMSF profiles of both free HDAC1 enzyme (in black) and the complexes formed by binding of the ligands **2a** (in blue), **6b** (in green) and **13** (in red) to HDAC1.

The difference between the values (~0.01–0.02 Å for HDAC1-ligand complexes and ~0.1–0.2 Å for mTOR-ligand complexes) may be neglected because this much differences (a little more stable association in the case of mTOR complexes) may not cause any significant changes on the enzyme structures. However, the results provide clear evidence of small changes in the conformational state of the enzymes, and more importantly, our study is focusing more on the functions of ligands on the enzyme inhibitions rather than the small structural changes.

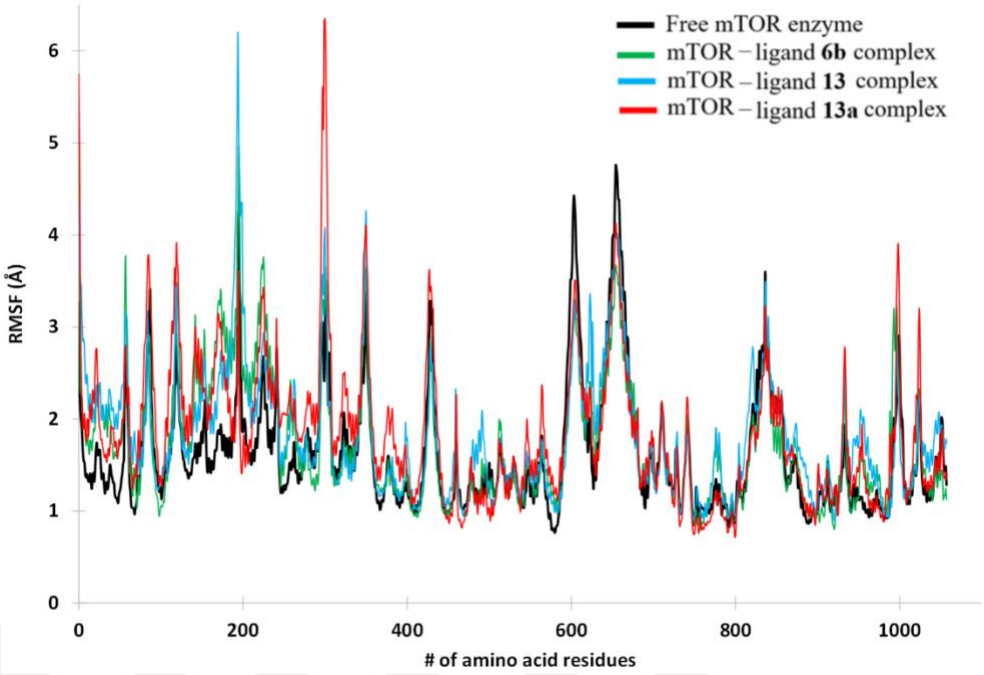


**Figure 3.7** The combined RMSF profiles of both free mTOR enzyme (in black) and the complexes formed by binding of the ligands **6b** (in green), **13** (in blue) and **13a** (in red) to mTOR.

In order to collect more information about overall dimensions, investigate the changes of the complex structures, and further analyze the compactness and rigidity of the enzyme-ligand complexes, the mass-weighted root-mean-square distance of a group of atoms from their typical center of mass (also known as radius of gyration (Rg) parameter [40]) has been calculated (**Figures 3.8** and **3.9**). From such values, consistency of the complex and consistent stability throughout the MD simulations can be predicted (the larger variations from the Rg indicates the inconsistency of the complexes [48]). The free enzymes HDAC1 and mTOR exhibit average Rg values of 1.376 and 1.383 nm (in black, **Figures 3.8** and **3.9**), respectively. In the case of HDAC1–ligand **6b** and mTOR–ligand **6b** complexes, the average Rg values are of 1.378 and 1.381 nm, respectively, and such values are slighly lower than the values exhibited by the free enzymes. This means the complexes have very smaller differences (almost negligible) than the free enzymes, referring to a little or almost no conformational changes throughout the MD simulations. A slight decrease in the average Rg values in each case elucidates higher compactnesses of the complexes, thereby suggesting higher stability and lower flexibility.

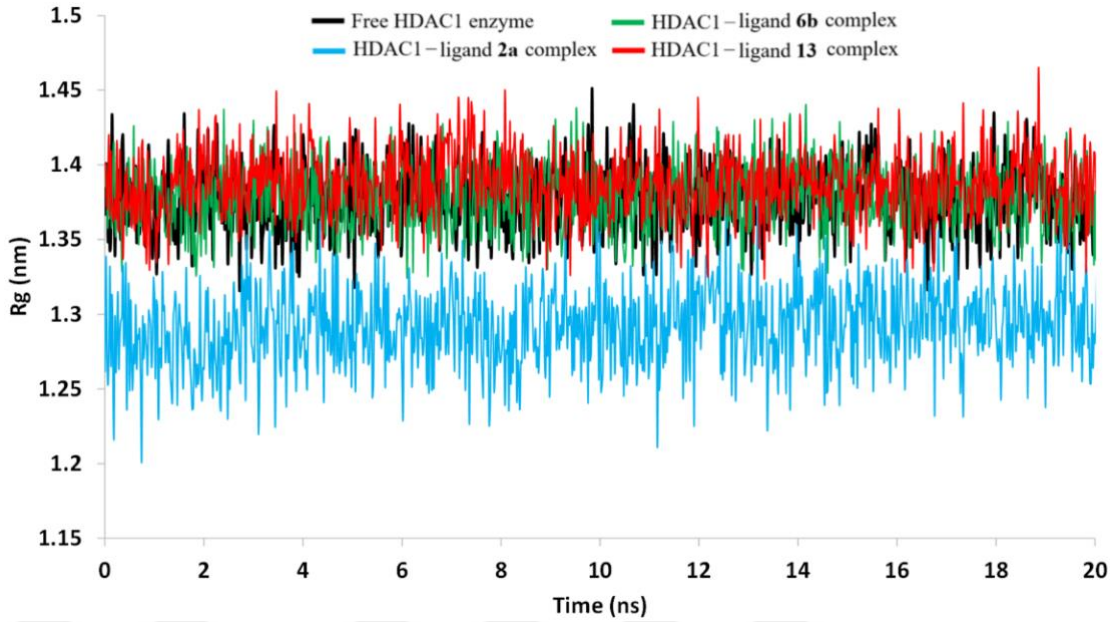


**Figure 3.8** The combined Rg profiles of both free HDAC1 enzyme (in black) and the complexes formed by binding of the ligands **2a** (in green), **6b** (in blue) and **13** (in red) to HDAC1.

For the average Rg values of the HDAC1–ligand **13** (1.389 nm, in red, **Figure 3.8**) and mTOR–ligand **13** (1.381 nm, in blue, **Figure 3.9**) complexes, the free HDAC1 enzyme exhibits lower Rg value than its pertinent complex with the ligand **13**, while mTOR–ligand **13** complex has lower average Rg value compared to its free enzyme mTOR. Although the smaller average Rg values denotes the higher compactness and stability with lower flexibility, the differences between the average Rg values of the free enzymes and complexes are still negligible. The HDAC1–ligand **2a** (1.293 nm, in blue, **Figure 3.8**) and mTOR–ligand **13a** (1.381 nm, in red, **Figure 3.9**) complexes also have lower average Rg values than their pertinent free enzymes, which suggest the higher compactness and stability with lower flexibility in these complexes as well.

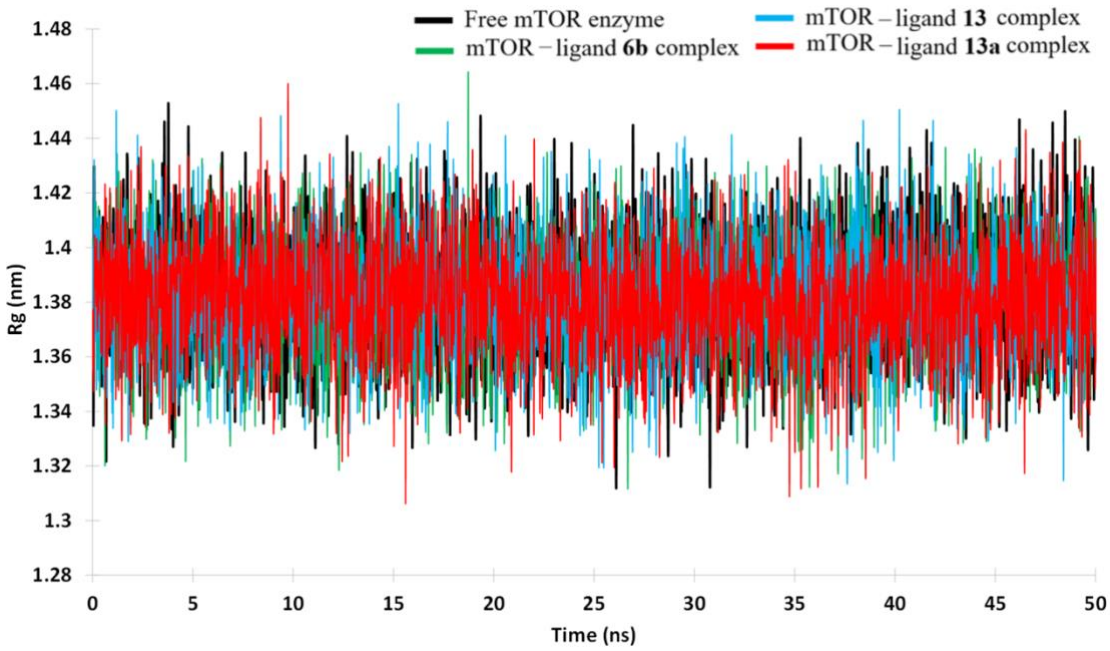


**Figure 3.9** The combined Rg profiles of both free mTOR enzyme (in black) and the complexes formed by binding of the ligands **6b** (in green), **13** (in blue) and **13a** (in red) to mTOR.

Since the chemical absorption, distribution, metabolism, excretion, and toxicity (ADMET, one of the most essential parts of computational drug design for the assessment of pharmacokinetics of a drug and/or an API) play key roles in drug discovery and development, an ADMET study by using a free web tool, SwissADME (with Lipinski's rule of five during the pre-clinical phase of drug discovery: Molecular Weight (MW) < 500, Number of Hydrogen Bond Donors ≤ 5, Number of Hydrogen Bond Acceptors ≤ 10, Calculated Log p ≤ 5, and Polar Surface Area (PSA) < 140 $Å^2$) [51], has been investigated (**Table 3.4**) for the most effective 20 ligands (**1**, **1a**, **1b**, **2**, **2a**, **2b**, **3**, **3b**, **5**, **5a**, **6b**, **7**, **7a**, **7b**, **8b**, **12b**, **13**, **13a**, **14b** and **23b**). The Lipinski's rule of five states that if a drug and/or an API violates more than two of the abovementioned criteria, it is considered impermeable or badly absorbed [51].

**Table 3.4** The ADMET study for the selected 20 ligands using a free web tool, SwissADME (with Lipinski's rule of five) [51].

| ADMET ANALYSIS | | | | | |
|---|---|---|---|---|---|
| **Ligand Name** | **Molecular Weight (g/mol)** | **Log P** | **H Bond Donor** | **H Bond Acceptor** | **Total Polar Surface Area (Å$^2$)** |
| **1** | 353.41 | 1.93 | 3 | 5 | 77.92 |
| **1a** | 383.44 | 1.87 | 3 | 6 | 87.15 |
| **1b** | 538.55 | 3.29 | 4 | 8 | 142.90 |
| **2** | 336.38 | 3.23 | 2 | 4 | 74.68 |
| **2a** | 366.41 | 3.23 | 2 | 5 | 83.91 |
| **2b** | 508.52 | 4.37 | 2 | 8 | 118.84 |
| **3** | 364.44 | 3.98 | 1 | 4 | 63.68 |
| **3b** | 508.52 | 4.37 | 2 | 8 | 118.84 |
| **5** | 316.32 | 4.65 | 1 | 4 | 28.15 |
| **5a** | 346.35 | 4.59 | 1 | 5 | 37.38 |
| **6b** | 468.39 | 7.17 | 0 | 8 | 25.78 |
| **7** | 293.3.2 | 3.00 | 1 | 3 | 73.97 |
| **7a** | 323.35 | 3.01 | 1 | 4 | 83.20 |
| **7b** | 500.39 | 6.79 | 0 | 10 | 44.27 |
| **8b** | 422.39 | 4.10 | 0 | 6 | 117.42 |
| **12b** | 584.71 | 4.11 | 0 | 4 | 72.88 |
| **13** | 437.58 | 4.51 | 3 | 2 | 55.45 |
| **13a** | 467.61 | 4.52 | 3 | 3 | 64.68 |
| **14b** | 710.91 | 6.74 | 4 | 4 | 80.38 |
| **23b** | 558.72 | 4.28 | 4 | 4 | 80.38 |

None of our abovelisted ligands violate more than two of the Lipinski's rule of five criteria, which provides a very promising and higher tendency for all ligands to pharmacologically be active (great API potents). Of the ligands, 12 of them (**1**, **1a**, **2**, **2a**,

**3**, **5**, **5a**, **7**, **7a**, **8b**, **13** and **13a**) completely meet all the criteria of Lipinski's rule of five. As stated above, the ligands **2a**, **6b** and **13** against the HDAC1 and **6b**, **13** and **13a** against the mTOR enzymes have exhibited very promising binding energies and inhibition constants from the docking processes with supporting MD simulations for the respective complexes. Except for the ligand **6b** (Log P = 7.17), ligands **2a**, **13** and **13a** also meet all the Lipinski's rule of five criteria.

Considering all the above findings with the supported literature details, synthetic possibility of the ligands have also been investigated and some general synthetic protocols utilizing and/more modifying the literature [38,52–62] have been proposed (**Figure 3.10**: **(A)** for the Ps-based derivatives from the **Figures 1.1A** and **1.1B**, and **Table 3.1**; **(B)** for the Ps derivatives from the **Figures 1.1C** and **1.1D**, and **Table 3.2**; and **(C)** for the PHEN-based derivatives from the **Figures 1.1E** and **1.1F**, and **Table 3.3**) in order to further obtain such ligands. Upon synthesis of the each promising ligand, their copper(I) complexes will be obtained by mixing 2:1 ratio of the relevant ligand and $[Cu(CH_3CN)_4]PF_6$ salt in the 1:1 mixture of dichloromethane and acetonitrile solvents. Such copper(I) complexes will also be further investigated.

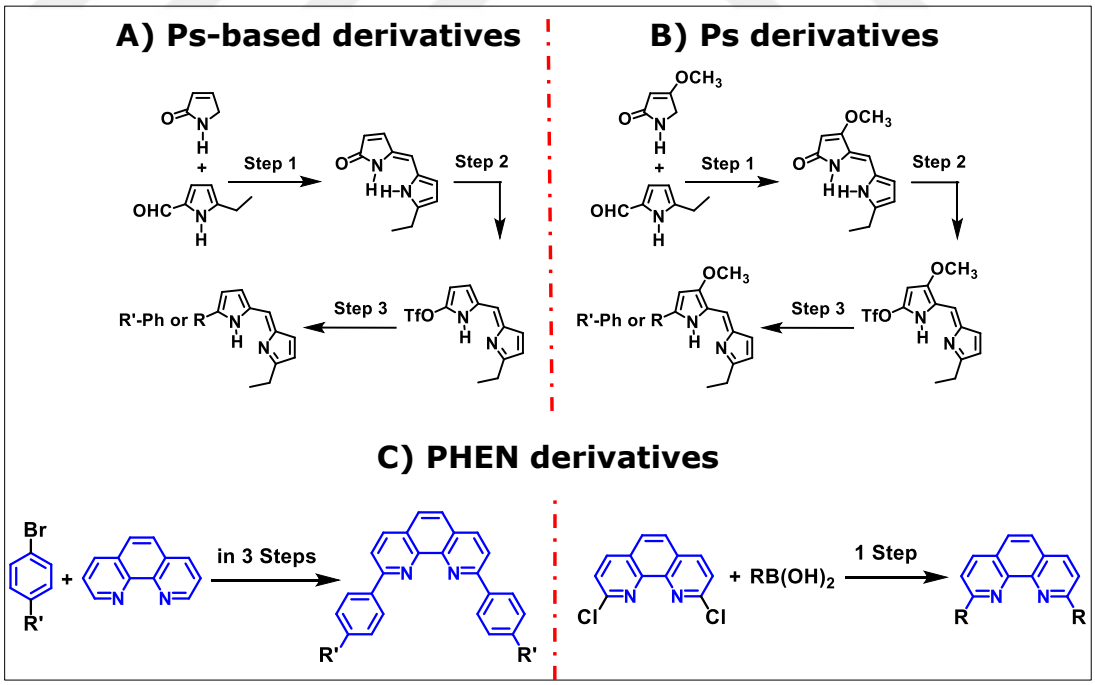


**Figure 3.10** The proposed general synthetic routes for the syntheses of (**A**) Ps-based, (**B**) Ps, and (**C**) PHEN derivatives from either literature or adapted procedures [38,52–62].

# 4. CONCLUSION

In conclusion, the structure-activity relationship and *in silico* modeling of a series of 1,10-phenanthroline and prodigiosin derivatives (75 in total) as highly potent and effective new anticancer therapeutic drug/API candidates against mTOR and HDAC enzymes have been investigated. Some of the designed and optimized ligands via *in silico* computational modeling (**1**, **1a**, **1b**, **2**, **2a**, **2b**, **3**, **3b**, **5**, **5a**, **6b**, **7**, **7a**, **7b**, **8b**, **12b**, **13**, **13a**, **14b** and **23b**) have exhibited very promising binding energies and inhibition constants against HDAC1 and/or mTOR enzymes after formation of the relative enzyme-ligand complexes. Such ligands have been found to be highly potent to inhibit either or both enzymes against brain metastatic breast cancer, preferentially against both for the dual action purposes. Compared to the natural product Ps, such proposed structures have exhibited effectiveness on inhibition of enzymes at nM level with very promising binding energies. While the ligands **6b** and **7b** have been showing very promising dual action against both of the enzymes from the PHEN derivatives, **2a**, **5** and **13** are the effective ones exhibiting dual action from the Ps-based and Ps derivatives. The further MD simulations for the selected ligands (**2a**, **6b** and **13** against HDAC1 and **6b**, **13** and **13a** against mTOR) exhibiting the best results regarding the binding energies and inhibition constants have also been conducted, and the parameters have been calculated from the trajectory of MD simulations, which have provided highly supporting evidence regarding structural conformations, stability of the enzyme backbone upon complex formation, consistent stability throughout the simulation, flexibility/fluctuation of the complexes, changes in complex structure and information about overall dimensions of complexes. All the complexes against both enzymes have exhibited higher RMSD values, referring to the presence of high degree of rotatable bonds or structural flexibilities that cause the ligands to be unable to attain stability inside the binding pocket of the enzymes, which are assumed to be shallow. When RMSF values are compared, the free enzymes have exhibited lower RMSFs than their relevant complexes with the selected ligands. Thus, the results have shown that the complexes have higher level of fluctuation patterns than the free enzymes, indicating that the residues are located in the loop regions with more conformational flexibility in the complexes rather than more constrained dynamics. The

outcomes from the RMSFs support that the free enzymes demonstrate restricted movements during the simulations as well. According to the calculated average Rg values, very small differences in the compared values for the free enzymes and complexes refer to a little or almost no conformational changes throughout the MD simulations in all cases. Slight decreases in the values have elucidated higher compactnesses of the structures, thereby suggesting higher stability and lower flexibility. The ADMET study using SwissADME (with Lipinski's rule of five) have provided that none of the selected ligands have violated more than two of the Lipinski's rule of five criteria, proving a highly promising tendency for the ligands to be pharmacologically active. Thus, we have acquired some compounds through *in silico* computational modeling that may provide great therapeutic potential for the breast cancer patients who are at a large brain metastasis risk. Considering highly promising outcomes of this work, further syntheses of some of the selected compounds are still under study in our laboratories.

# 5. REFERENCES


[1]. World Health Organization (WHO). *Breast cancer*. World Health Organization 2020; https://www.who.int/news-room/fact-sheets/detail/breast-cancer (accessed 2023-09-13).

[2]. BW, S.; CP, W. *World Cancer Report 2014*. https://publications.iarc.fr/Non-Series-Publications/World-Cancer-Reports/World-Cancer-Report-2014 (accessed 2023-09-13).

[3]. (a) Forman D.; Ferlay J.; *The global and regional burden of cancer. In: World Cancer Report 2014*, Stewart BW.; Wild CP; Eds.; International Agency for Research on Cancer 2014; 16-53; (b) Siegel, R. L.; Miller, K. D.; Jemal, A. Cancer statistics, 2020. *CA Cancer J. Clin.* **2020**, 70 (1), 7–30. DOI: 10.3322/caac.21590; (c) Al-Shamsi, H. O.; Alrawi, S. Breast Cancer Screening in the United Arab Emirates: Is It Time to Call for a Screening at an Earlier Age? *J. Cancer Prev. Curr. Res.* **2018**, *9* (3). DOI: 10.15406/jcpcr.2018.09.00334.

[4]. Leone, J. P.; Leone, B. A. Breast Cancer Brain Metastases: The Last Frontier. *Exp. Hematol. Oncol.* **2015**, *4* (1). DOI: 10.1186/s40164-015-0028-8.

[5]. Pangeni, R. P.; Channathodiyil, P.; Huen, D. S.; Eagles, L. W.; Johal, B. K.; Pasha, D.; Hadjistephanou, N.; Nevell, O.; Davies, C. L.; Adewumi, A. I.; Khanom, H.; Samra, I. S.; Buzatto, V. C.; Chandrasekaran, P.; Shinawi, T.; Dawson, T. P.; Ashton, K. M.; Davis, C.; Brodbelt, A. R.; Jenkinson, M. D. The GALNT9, BNC1 and CCDC8 Genes Are Frequently Epigenetically Dysregulated in Breast Tumours That Metastasise to the Brain. *Clin. Epigenetics* **2015**, *7* (1). DOI: 10.1186/s13148-015-0089-x.

[6]. Engel, J.; Eckel, R.; Aydemir, Ü.; Aydemir, S.; Kerr, J.; Schlesinger-Raab, A.; Dirschedl, P.; Hölzel, D. Determinants and Prognoses of Locoregional and Distant Progression in Breast Cancer. *Int. J. Radiat. Oncol. Biol. Phys.* **2003**, *55* (5), 1186–1195. DOI: 10.1016/s0360-3016(02)04476-0.

[7]. Rostami, R.; Mittal, S.; Rostami, P.; Tavassoli, F.; Jabbari, B. Brain Metastasis in Breast Cancer: A Comprehensive Literature Review. *J. Neurooncol.* **2016**, *127* (3),

407–414. DOI: 10.1007/s11060-016-2075-3.

[8]. (a) Kölbl, A. C.; Andergassen, U.; Jeschke, U. The Role of Glycosylation in Breast Cancer Metastasis and Cancer Control. *Front. Oncol.* **2015**, *5*. DOI: 10.3389/fonc.2015.00219; (b) Lin, S.; Kemmner W.; Grigull, S.; Schlag, P. M. Cell Surface alpha 2,6-Sialylation Affects Adhesion of Breast Carcinoma Cells. *Exp. Cell Res.* **2002**, *276* (1), 101–110. DOI: 10.1006/excr.2002.5521.

[9]. Godone, R. L. N.; Leitão, G. M.; Araújo, N. B.; Castelletti, C. H. M.; Lima-Filho, J. L.; Martins, D. B. G. Clinical and Molecular Aspects of Breast Cancer: Targets and Therapies. *Biomed. Pharmacother.* **2018**, *106*, 14–34. DOI: /10.1016/j.biopha.2018.06.066.

[10]. ASCO. *Breast Cancer*. https://www.cancer.net/cancer-types/breast-cancer/types-treatment (accessed 2023-09-19).

[11]. Alkabban, F. M.; Ferguson, T. *Breast Cancer*. National Library of Medicine. https://www.ncbi.nlm.nih.gov/books/NBK482286/ (accessed 2023-09-19).

[12]. Jin, X.; Mu, P. Targeting Breast Cancer Metastasis. *Breast Cancer: Basic Clin. Res.* **2015**, *9s1*, BCBCR.S25460. DOI: 10.4137/bcbcr.s25460

[13]. Sun, Y.-S.; Zhao, Z.; Yang, Z.-N.; Xu, F.; Lu, H.-J.; Zhu, Z.-Y.; Shi, W.; Jiang, J.; Yao, P.-P.; Zhu, H.-P. Risk Factors and Preventions of Breast Cancer. *Int. J. Biol. Sci.* **2017**, *13* (11), 1387–1397. DOI: 10.7150/ijbs.21635.

[14]. National Cancer Institute. *Breast Cancer Prevention*. National Cancer Institute, 2023. https://www.cancer.gov/types/breast/patient/breast-prevention-pdq (accessed 2023-09-19).

[15]. Al-Amri, A. M. Prevention of Breast Cancer. *J. Fam. Community Med.* **2005**, *12* (2), 71–74.

[16]. Sauter, E. R. Breast Cancer Prevention: Current Approaches and Future Directions. *Eur. J. Breast Health* **2018**, *14* (2). DOI: 10.5152/ejbh.2018.3978.

[17]. (a) Knight, Z. A.; Gonzalez, B.; Feldman, M. E.; Zunder, E. R.; Goldenberg, D. D.; Williams, O.; Loewith, R.; Stokoe, D.; Balla, A.; Toth, B.; Balla, T.; Weiss, W. A.; Williams, R. L.; Shokat, K. M. A Pharmacological Map of the PI3-K Family Defines a Role for P110α in Insulin Signaling. *Cell* **2006**, *125* (4), 733–747. DOI: 10.1016/j.cell.2006.03.035.; (b) Porta, C.; Paglino, C.; Mosca, A. Targeting

PI3K/Akt/MTOR Signaling in Cancer. *Front. Oncol.* **2014**, *4* (64). DOI: 10.3389/fonc.2014.00064.

[18]. Maiese, K. *Molecules to Medicine with mTOR: Translating Critical Pathways Into Novel Therapeutic Strategies. Cellular and Molecular Signaling.* Newark, NJ, USA Academic Press, Elsevier, 2016. DOI: 10.1016/C2014-0-03321-7

[19]. Seto, E.; Yoshida, M. Erasers of Histone Acetylation: The Histone Deacetylase Enzymes. *Cold Spring Harb. Perspect. Biol.* **2014**, *6* (4), a018713–a018713. DOI: 10.1101/cshperspect.a018713

[20]. Yao, D.; Jiang, J.; Zhang, H.; Huang, Y.; Huang, J.; Wang, J. Design, Synthesis and Biological Evaluation of Dual MTOR/HDAC6 Inhibitors in MDA-MB-231 Cells. *Bioorganic Med. Chem. Lett.* **2021**, *47*, 128204. DOI: 10.1016/j.bmcl.2021.128204.

[21]. Min, K.-N.; Joung, K.-E.; Kim, D.-K.; Sheen, Y.-Y. Anti-Cancer Effect of IN-2001 in MDA-MB-231 Human Breast Cancer. *Biomol. Ther.* **2012**, *20* (3), 313–319. DOI: 10.4062/biomolther.2012.20.3.313.

[22]. Guo, Q.; Cheng, K.; Wang, X.; Li, X.; Yu, Y.; Hua, Y.; Yang, Z. Expression of HDAC1 and RBBP4 Correlate with Clinicopathologic Characteristics and Prognosis in Breast Cancer. *Int. J. Clin. Exp. Pathol.* **2020**, *13* (3), 563–572.

[23]. Bian, X.; Liang, Z.; Feng, A.; Salgado, E.; Shim, H. HDAC Inhibitor Suppresses Proliferation and Invasion of Breast Cancer Cells through Regulation of MiR-200c Targeting CRKL. *Biochem. Pharmacol.* **2018**, *147*, 30–37. DOI: 10.1016/j.bcp.2017.11.008.

[24]. Tang, Z.; Ding, S.; Huang, H.; Luo, P.; Qing, B.; Zhang, S.; Tang, R. HDAC1 Triggers the Proliferation and Migration of Breast Cancer Cells via Upregulation of Interleukin-8. *Biol. Chem.* **2017**, *398* (12), 1347–1356. DOI: 10.1515/hsz-2017-0155.

[25]. Kawai, H.; Li, H.; Avraham, S.; Jiang, S.; Avraham, H. K. Overexpression of Histone Deacetylase HDAC1 Modulates Breast Cancer Progression by Negative Regulation of Estrogen Receptor α. *Int. J. Cancer* **2003**, *107* (3), 353–358. DOI: 10.1002/ijc.11403.

[26]. Fasolo, A.; Sessa, C. Targeting MTOR Pathways in Human Malignancies. *Curr. Pharm. Des.* **2012**, *18* (19), 2766–2777. DOI: 10.2174/138161212800626210.

[27]. Lu, Y.; Liu, W. Selective Estrogen Receptor Degraders (SERDs): A Promising Strategy for Estrogen Receptor Positive Endocrine-Resistant Breast Cancer. *J. Med. Chem.* **2020**, *63* (24), 15094–15114. DOI: 10.1021/acs.jmedchem.0c00913.

[28]. (a) Fricker, S. P. *Metal Compounds in Cancer Therapy*, 1st ed.; Springer Netherlands: Chapman and Hall, 1994. DOI: 10.1007/978-94-011-1252-9; (b) Heffeter, P.; Jakupec, M. A.; Körner, W.; Wild, S.; Keyserlingk, N. G.; Elbling, L.; Zorbas, H.; Korynevska, A.; Siegfried, K.; Sutterlüty, H.; Micksche, M.; Keppler, B. K.; Berger, W. Anticancer activity of the lanthanum compound [tris(1,10-phenanthroline)lanthanum(III)]trithiocyanate (KP772; FFC24). *Biochem. Pharmacol.* **2006**, *71* (4), 426–440. DOI: 1016/j.bcp.2005.11.009; (c) Zhang, C. X.; Lippard, S. J. New Metal Complexes as Potential Therapeutics. *Curr. Opin. Chem. Biol.* **2003**, *7* (4), 481–489. DOI: 10.1016/s1367-5931(03)00081-4.; (d) Marzano, C.; Trevisan, A.; Giovagnini, L.; Fregona, D. Synthesis of a New Platinum(II) Complex: Anticancer Activity and Nephrotoxicity in Vitro. *Toxicol. Vitro* **2002**, *16* (4), 413–419. DOI: 10.1016/s0887-2333(02)00022-x; (e) Ranford, J. D.; Sadler, P. J.; Tocher, D. A. Cytotoxicity and antiviral activity of transition-metal salicylato complexes and crystal structure of Bis(diisopropylsalicylato)(1,10-phenanthroline)copper(II). *J. Chem. Soc., Dalton Trans.* **1993**, 3393-3399. DOI: 10.1039/DT9930003393; (f) Saha, D.; Sandbhor, U.; K. Shirisha; Padhyé, S.; Deobagkar, D. N.; Anson, C. E.; Powell, A. K. A Novel Mixed-Ligand Antimycobacterial Dimeric Copper Complex of Ciprofloxacin and Phenanthroline. *Bioorganic Med. Chem. Lett.* **2004**, *14* (12), 3027–3032. DOI: 10.1016/j.bmcl.2004.04.043; (g) Zoroddu, M. A.; Zanetti, S.; Pogni, R.; Basosi, R. An Electron Spin Resonance Study and Antimicrobial Activity of Copper(II)-Phenanthroline Complexes. *J. Inorg. Biochem.* **1996**, *63* (4), 291–300. DOI: 10.1016/0162-0134(96)00015-3; (h) Erkkila, K. E.; Odom, D. T.; Barton, J. K. Recognition and Reaction of Metallointercalators with DNA. *Chem. Rev.* **1999**, *99* (9), 2777–2796. DOI: 10.1021/cr9804341; (i) Butler, H. M.; Hurse, A.; Thursky, E.; Shulman, A. Bactericidal action of selected phenanthroline chelates and related compounds. *Aust. J. Exp. Biol. Med. Sci.* **1969**, *47*(5), 541–552. DOI: 10.1038/icb.1969.148; (j) Macleod, R. A. The toxicity of o-phenanthroline for lactic acid bacteria. *J. Biol. Chem.* **1952**, *197*(2), 751–761. DOI: 10.1016/S0021-9258(18)55631-3; (k) Dwyer, F.; Reid, I. K.; Shulman, A.; Laycock, G. M.; Dixson,

S. The biological actions of 1,10-phenanthroline and 2,2'-bipyridine hydrochlorides, quaternary salts and metal chelates and related compounds: 1. Bacteriostatic action on selected gram-positive, gram-negative and acid-fast bacteria. *Aust. J. Exp. Biol. Med. Sci.* **1969**, *47*(2), 203–218. DOI: 10.1038/icb.1969.21; (l) Walsh, C. T.; Garneau-Tsodikova, S.; Howard-Jones, A. R. Biological Formation of Pyrroles: Nature's Logic and Enzymatic Machinery. *Nat. Prod. Rep.* **2006**, *23* (4), 517. DOI: 10.1039/b605245m; (m) Danevčič, T.; Borić Vezjak, M.; Zorec, M.; Stopar, D. Prodigiosin - a Multifaceted Escherichia Coli Antimicrobial Agent. *PLoS ONE* **2016**, *11* (9), e0162412. DOI: 1371/journal.pone.0162412; (n) Espona-Fiedler, M.; Soto-Cerrato, V.; Hosseini, A.; Lizcano, J. M.; Guallar, V.; Quesada, R.; Gao, T.; Pérez-Tomás, R. Identification of Dual MTORC1 and MTORC2 Inhibitors in Melanoma Cells: Prodigiosin vs. Obatoclax. *Biochem. Pharmacol.* **2012**, *83* (4), 489–496. DOI: 10.1016/j.bcp.2011.11.027; (o) Wang, Z.; Li, B.; Zhou, L.; Yu, S.; Su, Z.; Song, J.; Sun, Q.; Sha, O.; Wang, X.; Jiang, W.; Willert, K.; Wei, L.; Carson, D. A.; Lu, D. Prodigiosin Inhibits Wnt/β-Catenin Signaling and Exerts Anticancer Activity in Breast Cancer Cells. *Proc. Natl. Acad. Sci. U.S.A* **2016**, *113* (46), 13150–13155. DOI: 10.1073/pnas.1616336113; (p) Müller, B. M.; Jana, L.; Kasajima, A.; Lehmann, A.; Prinzler, J.; Budczies, J.; Winzer, K.-J.; Dietel, M.; Weichert, W.; Denkert, C. Differential Expression of Histone Deacetylases HDAC1, 2 and 3 in Human Breast Cancer - Overexpression of HDAC2 and HDAC3 Is Associated with Clinicopathological Indicators of Disease Progression. *BMC Cancer* **2013**, *13* (1). DOI: 10.1186/1471-2407-13-215; (q) de Ruijter A. J. M.; van Gennip A.H.; Caron H. N.; Kemp S.; van Kuilenburg A. B. P. Histone deacetylases (HDACs): characterization of the classical HDAC family. *Biochem. J.* **2003**, *370*(3), 737–749. DOI: 10.1042/bj20021321; (r) Weichert, W. HDAC expression and clinical prognosis in human malignancies. *Cancer Lett.* **2009**, *280*(2), 168–176. DOI: 10.1016/j.canlet.2008.10.047; (s) Shouksmith, A. E.; Gawel, J. M.; Nabanita Nawar; Sina, D.; Raouf, Y. S.; Bukhari, S.; He, L.; Johns, A. E.; Manaswiyoungkul, P.; Olasunkanmi, O. O.; Cabral, A. D.; Sedighi A.; de Araujo E. D.; Gunning, P. T. Class I/IIb-Selective HDAC Inhibitor Exhibits Oral Bioavailability and Therapeutic Efficacy in Acute Myeloid Leukemia. *ACS Med. Chem. Lett.* **2019**, *11*(1), 56–64. DOI: 10.1021/acsmedchemlett.9b00471; (t) Senese, S.; Zaragoza, K.; Minardi, S.;

Muradore, I.; Ronzoni, S.; Passafaro, A.; Bernard, L.; Draetta G. F.; Alcalay, M.; Seiser, C.; Chiocca, S. Role for Histone Deacetylase 1 in Human Tumor Cell Proliferation. *Mol. Cell. Biol.* **2007**, *27*(13), 4784–4795. DOI: 10.1128/mcb.00494-07; (u) Choi, J. H.; Kwon, H. J.; Yoon, B. I.; Kim J. H.; Han, S. U.; Joo, H. J.; Kim, D. Y. Expression Profile of Histone Deacetylase 1 in Gastric Cancer Tissues. *Jpn. J. Cancer Res.* **2001**, *92*(12), 1300–1304. DOI: 10.1111/j.1349-7006.2001.tb02153.x; (v) Halkidou, K.; Gaughan, L.; Cook, S.; Leung, H. Y.; Neal, D. E.; Robson, C. N. Upregulation and Nuclear Recruitment of HDAC1 in Hormone Refractory Prostate Cancer. *The Prostate* **2004**, *59*(2), 177–189. DOI: 10.1002/pros.20022; (w) Krusche, C. A.; Wülfing, P.; Kersting, C.; Vloet, A. J.; Böcker, W.; Kiesel, L.; Beier, H. M.; Alfer, J. Histone Deacetylase-1 and -3 Protein Expression in Human Breast Cancer: A Tissue Microarray Analysis. *Breast Cancer Res. Treat.* **2005**, *90*(1), 15–23. DOI: 10.1007/s10549-004-1668-2; (x) Uba, A. I.; Yelekçi, K. Identification of Potential Isoform-Selective Histone Deacetylase Inhibitors for Cancer Therapy: A Combined Approach of Structure-Based Virtual Screening, ADMET Prediction and Molecular Dynamics Simulation Assay. *J. Biomol. Struct. Dyn.* **2017**, *36*(12), 3231–3245. DOI: 10.1080/07391102.2017.1384402.

[29]. (a) Denoyer, D.; Masaldan, S.; Fontaine, S. L.; Cater, M. A. Targeting Copper in Cancer Therapy: 'Copper That Cancer' *Metallomics* **2015**, *7*(11), 1459–1476. DOI: 10.1039/C5MT00149H; (b) Ge, E. J.; Bush, A. I.; Casini, A.; Cobine, P. A.; Cross, J. R.; DeNicola, G. M.; Dou, Q. P.; Franz, K. J.; Gohil, V. M.; Gupta, S.; Kaler, S. G.; Lutsenko, S.; Mittal, V.; Petris, M. J.; Polishchuk, R.; Ralle, M.; Schilsky, M. L.; Tonks, N. K.; Vahdat, L. T.; Aelst, L. V. Connecting Copper and Cancer: From Transition Metal Signalling to Metalloplasia. *Nat. Rev. Cancer* **2022**, *22*(2), 102–113. DOI: 10.1038/s41568-021-00417-2; (c) Chang, CJ. Searching for harmony in transition-metal signalling. *Nat. Chem. Biol.* **2015**, *11*(10) 744–747. DOI: 10.1038/nchembio.1913; (d) Brady, D. C.; Crowe, M. S.; Turski, M. L.; Hobbs, G. A.; Yao, X.; Chaikuad, A.; Knapp, S.; Xiao, K.; Campbell, S. L.; Thiele, D. J.; Counter, C. M. Copper Is Required for Oncogenic BRAF Signalling and Tumorigenesis. *Nature* **2014**, *509*(7501), 492–496. DOI: 10.1038/nature13180; (e) Que, E. L.; Domaille, D. W.; Chang, C. J. Metals in Neurobiology: Probing Their Chemistry and Biology with Molecular Imaging. *Chem. Rev.* **2008**, *108*(5), 1517–

1549. DOI: 10.1021/cr078203u; (f) Solomon, E. I.; Sundaram, U. M.; Machonkin, T. E. Multicopper Oxidases and Oxygenases. *Chem. Rev.* **1996**, *96*(7), 2563–2606. DOI: 10.1021/cr950046o.; (g) Lippard, S. J.; Berg, J. M. *Principles of bioinorganic chemistry*. Mill Valley, CA, USA: University Science Books, 1994. DOI: 10.1016/0307-4412(95)90685-1; (h) Hanahan, D.; Weinberg, R. A. Hallmarks of Cancer: The next Generation. *Cell* **2011**, *144*(5), 646–674. DOI: 10.1016/j.cell.2011.02.013; (i) Li, Y. Copper Homeostasis: Emerging Target for Cancer Treatment. *IUBMB Life* **2020**, *72*(9), 1900–1908. DOI: 10.1002/iub.2341.

[30]. Huang, X.; Hou, Y.; Weng, X.; Pang, W.; Hou, L.; Liang, Y.; Wang, Y.; Du, L.; Wu, T.; Yao, M.; Wang, J.; Meng, X. Diethyldithiocarbamate-Copper Complex (CuET) Inhibits Colorectal Cancer Progression via MiR-16-5p and 15b-5p/ALDH1A3/PKM2 Axis-Mediated Aerobic Glycolysis Pathway. *Oncogenesis* **2021**, *10*(1). DOI: 10.1038/s41389-020-00295-7.

[31]. Hussain, A.; AlAjmi, M. F.; Rehman, M. T.; Amir, S.; Husain, F. M.; Alsalme, A.; Siddiqui, M. A.; AlKhedhairy, A. A.; Khan, R. A. Copper(II) Complexes as Potential Anticancer and Nonsteroidal Anti-Inflammatory Agents: In Vitro and in Vivo Studies. *Sci. Rep.* **2019**, *9*(1), 1–17. DOI: 10.1038/s41598-019-41063-x.

[32]. Marzano, C.; Pellei, M.; Tisato, F.; Santini, C. Copper Complexes as Anticancer Agents. *Anti-Cancer Agents Med. Chem.* **2009**, *9*(2), 185–211. DOI: 10.2174/187152009787313837

[33]. Lumme, P.; Elo, H.; Jänne, J. Antitumor Activity and Metal Complexes of the First Transition Series. Trans-Bis(Salicylaldoximato)Copper(II) and Related Copper(II) Complexes, a Novel Group of Potential Antitumor Agents. *Inorganica Chim. Acta* **1984**, *92*(4), 241–251. DOI: 10.1016/s0020-1693(00)80045-6.

[34]. Molinaro, C.; Martoriati, A.; Pelinski, L.; Cailliau, K. Copper Complexes as Anticancer Agents Targeting Topoisomerases I and II. *Cancers* **2020**, *12*(10), 2863. DOI: 10.3390/cancers12102863.

[35]. (a) Zhang, Z.; Bi, C.; Fan, Y.; Zhang, N.; Deshmukh, R.; Yan, X.; Lv, X.; Zhang, P.; Zhang, X.; Dou, Q. P. L-Ornithine Schiff base-copper and -cadmium complexes as new proteasome inhibitors and apoptosis inducers in human cancer cells. *J. Biol. Inorg. Chem.* **2014**, *20*(1), 109–121. DOI: 10.1007/s00775-014-1219-1; (b) Hindo, S. S.; Frezza, M.; Tomco, D.; Heeg, M. J.; Hryhorczuk, L.; McGarvey, B. R.;

Dou, Q. P.; Verani, C. N. Metals in Anticancer Therapy: Copper(II) Complexes as Inhibitors of the 20S Proteasome. *Eur. J. Med. Chem.* **2009**, *44*(11), 4353–4361. DOI: 10.1016/j.ejmech.2009.05.019; (c) Zhang, Z.; Bi, C.; Schmitt, S. M.; Fan, Y.; Dong, L.; Zuo, J.; Dou, Q. P. 1,10-Phenanthroline Promotes Copper Complexes into Tumor Cells and Induces Apoptosis by Inhibiting the Proteasome Activity. *J. Biol. Inorg. Chem.* **2012**, *17*(8), 1257–1267. DOI: 10.1007/s00775-012-0940-x; (d) Zhang, X.; Bi, C.; Yu, F.; Cui Q. C.; Chen, D.; Xiao, Y.; Dou Q. P. Induction of tumor cell apoptosis by taurine Schiff base copper complex is associated with the inhibition of proteasomal activity. *Int. J. Mol. Med.* **2008**, *22*(5): 677–682. DOI: 10.3892/ijmm_00000072; (e) Zuo, J.; Bi, C.; Fan, Y.; Buac, D.; Nardon, C.; Daniel, K. G.; Dou, Q. P. Cellular and Computational Studies of Proteasome Inhibition and Apoptosis Induction in Human Cancer Cells by Amino Acid Schiff Base–Copper Complexes. *J. Inorg. Biochem.* **2013**, *118*, 83–93. DOI: 10.1016/j.jinorgbio.2012.10.006.

[36]. (a) Montaner, B.; Navarro, S.; Piqué, M.; Vilaseca, M.; Martinell, M.; Giralt, E.; Gil, J.; Pérez-Tomás, R. Prodigiosin from the Supernatant Of Serratia Marcescensinduces Apoptosis in Haematopoietic Cancer Cell Lines. *Br. J. Pharmacol.* **2000**, *131*(3), 585–593. DOI: 10.1038/sj.bjp.0703614; (b) Montaner, B.; Pérez-Tomás, R. Prodigiosin-Induced Apoptosis in Human Colon Cancer Cells. *Life Sci.* **2001**, *68*(17), 2025–2036. DOI: 10.1016/s0024-3205(01)01002-5; (c) Díaz-Ruiz, C.; Montaner, B.; Pérez-Tomás, R. Prodigiosin Induces Cell Death and Morphological Changes Indicative of Apoptosis in Gastric Cancer Cell Line HGT-1. *Histol. Histopathol.* **2001**, *16*(2), 415–421. DOI: 10.14670/hh-16.415; (d) Montaner, B.; Pérez-Tomás, R. The Prodigiosins: A New Family of Anticancer Drugs. *Curr. Cancer Drug Targets* **2003**, *3*(1), 57–65. DOI: 10.2174/1568009033333772.; (e) Soto-Cerrato, V.; Llagostera, E.; Montaner, B.; Scheffer, G. L.; Perez-Tomas, R. Mitochondria-Mediated Apoptosis Operating Irrespective of Multidrug Resistance in Breast Cancer Cells by the Anticancer Agent Prodigiosin. *Biochem. Pharmacol.* **2004**, *68*(7), 1345–1352. DOI: 10.1016/j.bcp.2004.05.056.

[37]. Rapoport, H.; Holden, K.G. The synthesis of prodigiosin. *J. Am. Chem. Soc.* **1960**, *82*(20), 5510–5511. DOI: 10.1021/ja01505a056

[38]. Cetin, M. M.; Peng, W.; Unruh, D.; Mayer, M. F.; Mechref, Y.; Yelekci K. Design, Synthesis, Molecular Modeling, and Bioactivity Evaluation of 1,10-Phenanthroline and Prodigiosin (Ps) Derivatives and Their Copper(I) Complexes against MTOR and HDAC Enzymes as Highly Potent and Effective New Anticancer Therapeutic Drugs. *Front. Pharmacol.* **2022**, *13*. DOI: 10.3389/fphar.2022.980479.

[39]. Morris, G. M.; Goodsell, D. S.; Halliday, R. S.; Huey, R.; Hart, W. E.; Belew, R. K.; Olson, A. J. Automated Docking Using a Lamarckian Genetic Algorithm and an Empirical Binding Free Energy Function. *J. Comput. Chem.* **1998**, *19*(14), 1639–1662. DOI: 1002/(sici)1096-987x(19981115)19:14%3C1639::aid-jcc10%3E3.0.co;2-b.

[40]. Studio D. Dassault Systemes BIOVIA, Discovery Studio Modelling Environment, Release 4.5. *Accelrys Software Inc.*, 2015. https://www.3ds.com/products/biovia/discovery-studio

[41]. Morris, G. M.; Huey, R.; Lindstrom, W.; Sanner, M. F.; Belew, R. K.; Goodsell, D. S.; Olson, A. J. AutoDock4 and AutoDockTools4: Automated Docking with Selective Receptor Flexibility. *J. Comput. Chem.* **2009**, *30*(16), 2785–2791. DOI: 10.1002/jcc.21256.

[42]. Akdoğan, E. D.; Erman, B.; Yelekci, K. In silico Design of Novel and Highly Selective Lysine-Specific Histone Demethylase Inhibitors. *Turk. J. Chem.* **2011**, *35*(4), 1–20. DOI: 10.3906/kim-1102-985

[43]. Eberhardt, J.; Santos-Martins, D.; Tillack, A. F.; Forli, S. AutoDock Vina 1.2.0: New Docking Methods, Expanded Force Field, and Python Bindings. *J. Chem. Inf. Model.* **2021**, *61*(8). DOI: 10.1021/acs.jcim.1c00203.

[44]. Phillips, J. C.; Braun, R.; Wang, W.; Gumbart, J.; Tajkhorshid, E.; Villa, E.; Chipot, C.; Skeel, R. D.; Kalé, L.; Schulten, K. Scalable Molecular Dynamics with NAMD. *J. Comput. Chem.* **2005**, *26*(16), 1781–1802. DOI: 10.1002/jcc.20289.

[45]. Jo, S.; Kim, T.; Iyer, V. G.; Im, W. CHARMM-GUI: A Web-Based Graphical User Interface for CHARMM. *J. Comput. Chem.* **2008**, *29*(11), 1859–1865. DOI: 10.1002/jcc.20945.

[46]. Sinnokrot, M. O.; Sherrill, C. D. Substituent Effects in π−π Interactions: Sandwich and T-Shaped Configurations. *J. Am. Chem. Soc.* **2004**, *126*(24), 7690–7697. DOI: 10.1021/ja049434a.

[47]. Kufareva, I.; Abagyan, R. Methods of Protein Structure Comparison. *Homology Modeling. Methods in Molecular Biology*; Orry, A.; Abagyan, R., Eds.; vol 857: 231–257. Clifton, NJ, USA: Humana Press, 2012. DOI: .1007/978-1-61779-588-6_10

[48]. Bhowmick, S.; AlFaris, N. A.; ALTamimi, J. Z.; ALOthman, Z. A.; Aldayel, T. S.; Wabaidur, S. M.; Islam, M. A. Screening and Analysis of Bioactive Food Compounds for Modulating the CDK2 Protein for Cell Cycle Arrest: Multi-Cheminformatics Approaches for Anticancer Therapeutics. *J. Mol. Struct.* **2020**, *1216*, 128316. DOI: 10.1016/j.molstruc.2020.128316.

[49]. Pereira G. R. C.; Vieira B. de. A. A.; De Mesquita, J. F. Comprehensive in silico analysis and molecular dynamics of the superoxide dismutase 1 (SOD1) variants related to amyotrophic lateral sclerosis. *PLoS One* **2021**, *16*(2), e0247841. DOI: 10.1371/journal.pone.0247841

[50]. Lobanov, M. Y.; Bogatyreva, N. S.; Galzitskaya, O. V. Radius of Gyration as an Indicator of Protein Structure Compactness. *Mol. Biol.* **2008**, *42*(4), 623–628. DOI: 10.1134/S0026893308040195.

[51]. Daina, A.; Michielin, O.; Zoete, V. SwissADME: A Free Web Tool to Evaluate Pharmacokinetics, Drug-Likeness and Medicinal Chemistry Friendliness of Small Molecules. *Sci. Rep.* **2017**, *7*(1). DOI: 10.1038/srep42717.

[52]. Dietrich-Buchecker, C.; Sauvage, J. Templated Synthesis of Interlocked Macrocyclic Ligands, the Catenands. Preparation and Characterization of the Prototypical Bis-30 Membered Ring System. *Tetrahedron* **1990**, *46*(2), 503–512. DOI: 10.1016/s0040-4020(01)85433-8.

[53]. Zhong, W.; Tang, Y.; Zampella, G.; Wang, X.; Yang, X.; Hu, B.; Wang, J.; Xiao, Z.; Wei, Z.; Chen, H.; Luca D. G.; Liu, X. A rare bond between a soft metal (FeI) and a relatively hard base (RO−, R = phenolic moiety). *Inorg. Chem. Commun.* **2010**, *13*(9), 1089–1092. DOI: 10.1016/j.inoche.2010.06.026

[54]. Kang, S.; Cetin, M. M.; Jiang, R.; Clevenger, E. S.; Mayer, M. F. Synthesis of Metalated Pseudorotaxane Polymers with Full Control over the Average Linear Density of Threaded Macrocycles. *J. Am. Chem. Soc.* **2014**, *136*(36), 12588–12591. DOI: 10.1021/ja507167k.

[55]. Cetin, M. M. Syntheses and characterization of copper(I) complexes for study of dynamic supramolecular ring-chain equilibria and application as photoredox

catalysts. Ph.D. Dissertation, Texas Tech University, Lubbock, TX, USA, 2017. https://ttu-ir.tdl.org/items/3e00e225-cd3b-41be-9348-d90b8df2f7d8 (accessed 2023-09-20)

[56]. Cetin, M. M.; Hodson, R. T.; Hart C. R.; Cordes, D. B.; Findlater, M.; Casadonte, D. J.; Cozzolino, A. F.; Mayer, M. F. Characterization and Photocatalytic Behavior of 2,9-Di(Aryl)-1,10-Phenanthroline Copper(I) Complexes. *Dalton Trans.* **2017**, *46*(20), 6553–6569. DOI: 10.1039/c7dt00400a.

[57]. Cetin, M. M.; Shafiei-Haghighi, S.; Chen, J.; Zhang, S.; Miller, A. C.; Unruh, D. K.; Casadonte, D. J.; Lohr, T. L.; Marks, T. J.; Mayer, M. F.; Stoddart, J. F.; Findlater, M. Synthesis, structures, photophysical properties, and catalytic characteristics of 2,9-dimesityl-1,10-phenanthroline (dmesp) transition metal complexes. *J. Polym. Sci.* **2020**, *58*(8), 1130–1143. DOI: 10.1002/pol.20190276

[58]. Schmittel, M.; Lüning, U.; Meder, M.; Ganz, A.; Michel, C.; Herderich, M. Synthesis of sterically encumbered 2,9-diaryl substituted phenanthrolines. Key building blocks for the preparation of mixed (Bis-heteroleptic) phenanthroline copper(I) complexes. *Heterocycl. Commun.* **1997**, *3*(6), 493–498. DOI: 10.1515/HC.1997.3.6.493

[59]. Kohler, L.; Hadt, R. G.; Hayes, D.; Chen, L. X.; Mulfort, K. L. Synthesis, Structure, and Excited State Kinetics of Heteroleptic Cu(I) Complexes with a New Sterically Demanding Phenanthroline Ligand. *Dalton Trans.* **2017**, *46*(38), 13088–13100. DOI: 10.1039/c7dt02476b.

[60]. Kohler, L.; Hayes, D.; Hong, J.; Carter, T. J.; Shelby, M. L.; Fransted, K. A.; Chen, L. X.; Mulfort, K. L. Synthesis, Structure, Ultrafast Kinetics, and Light-Induced Dynamics of CuHETPHEN Chromophores. *Dalton Trans.* **2016**, *45*(24), 9871–9883. DOI: 10.1039/c6dt00324a.

[61]. Hayes, D.; Kohler, L.; Chen, L. X.; Mulfort, K. L. Ligand Mediation of Vectorial Charge Transfer in Cu(I)Diimine Chromophore–Acceptor Dyads. *J. Phys. Chem. Lett.* **2018**, *9*(8), 2070–2076. DOI: 10.1021/acs.jpclett.8b00468.

[62]. Hayes, D.; Kohler, L.; Hadt, R. G.; Zhang, X.; Liu, C.; Mulfort, K. L.; Chen, L. X. Excited State Electron and Energy Relays in Supramolecular Dinuclear Complexes Revealed by Ultrafast Optical and X-Ray Transient Absorption Spectroscopy. *Chem. Sci.* **2018**, *9*(4), 860–875. DOI: 10.1039/c7sc04055e.

# CURRICULUM VITAE

**Personal Information**

Name and surname: Sümeyye Berfin Gül

**Academic Background**

| | |
|---|---|
| 2022 – 2024 | Master of Science in Material Science and Nanotechnology<br>Kadir Has University/ Istanbul/ Turkey |
| 2020 – 2022 | Teaching Assistant<br>Kadir Has University/ Istanbul/ Turkey |
| SUMMER 2021 | Internship in UGES Healthcare System Engineering<br>ASELSAN/ Ankara/ Turkey |
| SUMMER 2020 | Internship in Genetic Engineering and Biotechnology Institute<br>TUBITAK MAM/ Gebze/ Turkey |
| 2020 – 2022 | Minor Program in Computer Engineering<br>Kadir Has University/ Istanbul/ Turkey |
| 2017 – 2022 | Bachelor of Science in Bioinformatics and Genetics<br>Kadir Has University/ Istanbul/ Turkey |

| |
|---|
| Native Speaker in Turkish/ Fluent in English/ Beginner in German |
| Skills in molecular modelling in Autodock/VMD/Pymol/BIOVIA |
| Skills in programming languages in Python/Matlab |
| Skills in analytical techniques in UV-vis/MS |

**Work Experience**

| | |
|---|---|
| September 2021 – June 2022 | Undergraduate Course Teaching Asistant<br>Kadir Has University/ Istanbul/ Turkey<br>Numerical Methods and Optimization Techniques |
| September 2020 – June 2021 | Undergraduate Course Teaching Asistant<br>Kadir Has University/ Istanbul/ Turkey<br>Probability and Statistics for Engineers |

**Publications**

| |
|---|
| Polat, E. O.; Cetin, M. M.; Tabak, A. F.; Bilget Güven, E.; Uysal, B. Ö.; Arsan, T.; Kabbani, A.; Hamed, H.; **Gül, S. B**. Transducer Technologies for Biosensors and Their Wearable Applications. *Biosensors* **2022**, *12*(6), 385. DOI: 10.3390/bios12060385. |